

Updating intensity-duration-frequency curves for urban infrastructure design under a changing environment

Lei Yan¹  | Lihua Xiong² | Cong Jiang³ | Mengjie Zhang⁴ | Dong Wang⁵ | Chong-Yu Xu⁶

¹College of Water Conservancy and Hydropower, Hebei University of Engineering, Handan, China

²State Key Laboratory of Water Resources and Hydropower Engineering Science, Wuhan University, Wuhan, China

³School of Environmental Studies, China University of Geosciences (Wuhan), Wuhan, China

⁴Department of Earth and Environmental Engineering, Columbia University, New York, New York

⁵College of New Energy and Environment, Jilin University, Changchun, China

⁶Department of Geosciences, University of Oslo, Oslo, Norway

Correspondence

Lei Yan, College of Water Conservancy and Hydropower, Hebei University of Engineering, Handan 056021, China.
 Email: yanl@whu.edu.cn

Funding information

National Natural Science Foundation of China, Grant/Award Numbers: 51525902, 51809243, 51909053; Natural Science Foundation of Hebei Province, Grant/Award Number: E2019402076; Research Council of Norway, Grant/Award Numbers: FRINATEK Project 274310, KLIMAFORSK Project 302457; the Ministry of Education “Plan 111” Fund of China, Grant/Award Number: B18037; the Youth Foundation of Education Department of Hebei Province, Grant/Award Number: QN2019132

Edited by: Stuart N. Lane, Editor-in-Chief.

Abstract

The intensity and frequency of extreme precipitation have increased in many regions in the past century due to climate change. Many studies have revealed that short-duration extreme precipitations are likely to become more and more severe in many areas, thus raising a question on whether our urban infrastructures have been designed adequately to cope with these changes. Currently, Intensity–duration–frequency (IDF) curves, which summarize the relationships between the intensity and frequency of extreme precipitation for different durations, are recommended as a criterion for urban infrastructure design and stormwater management. However, climate change is thought to have invalidated the stationary assumption in deriving IDF curves, that is, current IDF curves could misestimate future extreme precipitation in many cases. Therefore, it is necessary to update the current IDF curves by considering possible changes of extreme precipitation. In this review, we first summarize observed changes in urban short-duration extreme precipitation and explore the physical mechanisms associated with changes. Then, we introduce two major approaches for updating IDF curves, namely the covariate-based nonstationary IDF curves and climate-model-based IDF curves. Advances in these two updating approaches for IDF curves are the focus of this review. These include the investigation of physically-based covariates with non-stationary modeling of extreme precipitation; nonstationary precipitation design strategies; and the statistical downscaling and dynamic downscaling methods for projecting future short-duration precipitation. Finally, we summarize some future research challenges and opportunities on providing reliable projections of future short-duration extreme precipitation and better characterize the probabilistic behavior of short-duration extreme precipitation for IDF design.

This article is categorized under:

Engineering Water > Engineering Water

KEY WORDS

climate change, extreme precipitation, intensity-duration-frequency curves, nonstationarity, urban infrastructure design

1 | INTRODUCTION

Over the past century, we have witnessed an increase in the global temperature as a result of human activities and associated anthropogenic greenhouse gas emissions (Hansen, Ruedy, Sato, & Lo, 2010; Meinshausen et al., 2009). The increasing temperature is expected to boost the saturation vapor pressure of air at a rate of approximately $7\text{ }^{\circ}\text{C}^{-1}$, governed by the Clausius–Clapeyron (C–C) equation (Feng et al., 2016; Guerreiro et al., 2018; Herath, Sarukkalige, & Nguyen, 2018; Lenderink & Fowler, 2017). A higher saturation vapor pressure is likely to increase the potential of water release (Ben Alaya, Zwiers, & Zhang, 2020; Chen, Hossain, & Leung, 2017; Kunkel et al., 2013), particularly for the short-duration extreme precipitation (Lenderink, Mok, Lee, & Van Oldenborgh, 2011; Liang & Ding, 2017). According to the Fifth Assessment Report (AR5) of Intergovernmental Panel on Climate Change (IPCC), the frequency and intensity of extreme precipitation are likely to increase in most land areas at the end of 21st century (IPCC, 2013). Relative to undeveloped and suburb regions, urban areas, particularly the densely-populated and highly-developed megacities are more sensitive to the impacts of climate change because of the complex effects of Urban Heat Island (UHI) on precipitation. On one hand, UHI increases the saturation vapor pressure of a given air mass and reduces its relative humidity. On the other hand, UHI may induce convective precipitation. Some clues regarding the impacts of urbanization on extreme precipitation have been published in recent decades (Agilan & Umamahesh, 2016; Golroudbary, Zeng, Mannaerts, & Su, 2019; Gu, Zhang, Li, Singh, & Sun, 2019; Lu et al., 2019; Miao, Sun, Borthwick, & Duan, 2016; Zhang, Villarini, Vecchi, & Smith, 2018). Moreover, at the local and global scales, many studies have reported the rising urban short-duration extreme precipitation in Europe, Asia, and America (Barbero, Fowler, Lenderink, & Blenkinsop, 2017; Jakob, Karoly, & Seed, 2011; Lenderink et al., 2011; Liang & Ding, 2017; Kan et al., 2016; Madsen, Arnbjerg-Nielsen, & Mikkelsen, 2009; Mishra, Ganguly, Nijssen, & Lettenmaier, 2015).

Currently, intensity–duration–frequency (IDF) curves are typically employed in urban infrastructure design and storm water management, with the purpose of reducing extreme precipitation and urban flooding issues. IDF curves are designed to reflect the statistical characteristics of precipitation and represent the relationships between intensity and frequency of precipitation for different durations. Precipitation intensities for different durations (e.g., 15-min, 30-min, 1-hr, 2-hr, 6-hr, 12-hr, and 24-hr) are estimated by fitting a theoretical probability distribution to annual maximum (AM) precipitation samples or peaks over threshold (POT) samples. Currently, the design concepts of IDF curves are mostly based on the stationary (ST) assumption. Under the ST condition, the statistical characteristics of extreme precipitation are assumed to be invariant over time, thus the probability distribution of extreme precipitation in the future period is expected to be identical to that in the historical period. However, the ST assumption has been challenged in recent decades because climate change and urbanization are expected to alter the local climate settings. Therefore, the statistical properties of precipitation cannot be considered as ST. In other words, the local extreme precipitation events could increase or decrease due to increased aridity. To cope with this challenge, the nonstationary (NS) assumption has been proposed in hydrology and climate-related literature (Hu et al., 2018; Kuang et al., 2018; Lu et al., 2019; Villarini, Serinaldi, Smith, & Krajewski, 2009; Vogel, Yaindl, & Walter, 2011; Xiong et al., 2019; Xiong et al., 2020; Xu, Jiang, Yan, Li, & Liu, 2018; Yan et al., 2019; Yan et al., 2020; Yan, Xiong, Liu, Hu, & Xu, 2017; Yang, Xiong, Xiong, Zhang, & Xu, 2020).

Under NS condition, the statistical parameters of probability distribution of extreme precipitation are no longer constant but can vary with covariate or time. This kind of changing statistical properties of extreme precipitation raises the question of whether the stationarity-based conventional design concepts of urban infrastructures are still adequate under changing environment. Given the observed increase in extreme precipitation at many places worldwide, some studies have recommended that the current IDF curves should be adapted to account for the impacts of climate change (Acero et al., 2017; Agilan & Umamahesh, 2017; Cheng & Aghakouchak, 2014; Ganguli & Coulibaly, 2017; Hassanzadeh, Nazemi, & Elshorbagy, 2014; Sarhadi & Soulis, 2017; Singh & Zhang, 2007; Westra et al., 2014;

Willem, 2013). In recent years, the NS frequency analysis has become one of the hot research topics in hydrology and climatology fields (Bayazit, 2015; Hao & Singh, 2016; Salas, Obeysekera, & Vogel, 2018). Moreover, more attention has been paid to the NS IDF curves to maintain the reliability of urban infrastructures and storm water management. In this article, we focus on the studies of construction of NS IDF curves. We aim to review the existing methods as well as discuss future research opportunities.

2 | URBAN SHORT-DURATION EXTREME PRECIPITATION

2.1 | Observed changes in urban short-duration extreme precipitation

Short-duration extreme precipitation generally refers to the extreme precipitation with sub-daily or sub-hourly durations. For decades, trend analysis has been routinely conducted on daily precipitation due to the scarcity and accessibility of short-duration extreme precipitation. However, many studies have suggested that the intensity of short-duration extreme precipitation is more pronounced than that of daily extreme precipitation (Westra et al., 2014), which will result in more hazardous flooding in urban areas. Therefore, it is essential to directly analyze the trend of urban short-duration precipitation to reveal the changing properties of urban short-duration extreme precipitation. Currently, trend analysis on extreme precipitation can be categorized into three groups:

- Trend detection in observed series. It involves collecting samples of AM precipitation or POT events with different durations, and calculating the trend in intensity of AM events or in frequency of POT events.
- Trend detection in extreme precipitation index (EPI). It first defines different EPIs, for example, 95th percentile of daily precipitation, days of extreme precipitation (days with precipitation larger than 95th percentile of daily precipitation), and heavy precipitation volume (total precipitation volume with daily precipitation greater than 95th percentile of daily precipitation in a year). Next, the trend of each EPI is analyzed.
- Stationarity tests based on split-sample tests. These are performed by splitting the entire historical precipitation data into sequential subsets and estimating the design precipitation or IDF curves for each subset. Finally, the change of design precipitation or IDF curves is analyzed.

Table 1 summarizes some studies on trend analysis of urban short-duration extreme precipitation using historical observation data. For example, Agilan and Umamahesh (2015) examined the trend of 4-hr extreme precipitation of Hyderabad, India. They first defined four EPIs for sub-daily precipitation, namely the annual number of days when precipitation >10 mm during corresponding 4 hr and season (R10-4hr), annual number of days when precipitation >20 mm during corresponding 4 hr and season (R20-4 hr), annual total precipitation from days >95 th percentile rainfall of corresponding 4 hr and season (R95p-4 hr), and annual total precipitation from days >1 mm during corresponding 4 hr and season (PRCPTOT-4 hr). Then, the changes of the four EPIs were fitted using linear regression method and the statistical significance was tested using the *F*-test. It was found that, generally, the frequency and intensity of 4-hr extreme precipitation have increased during the monsoon seasons. Moreover, the trend of extreme precipitation occurred between 1 and 4 a.m. was more significant than others, and the intensity of extreme precipitation that occurred between 9 p.m. and 12 a.m. was greater than other time periods. Besides, Agilan and Umamahesh (2017) examined the trends of AM series with 2, 3, 6, 12, 18, 24, 36, and 48 hr durations, and found that all the AM series exhibited significant increasing trends at the 5% significance level except 1 hr duration (Figure 1). Notably, these intensities were probably very much dependent of each other. Similarly, the increase of intensity and frequency of urban short-duration extreme precipitation was observed and identified in many cities, although several cities exhibited the opposite trend. In addition, the variability of trends of urban short-duration extreme precipitation is related to the duration over which the cumulated rainfall is considered and occurrence seasons. Thus, the trends can vary from site to site due to sampling variability.

2.2 | Physical mechanism associated with extreme precipitation

It is crucial to investigate the physical mechanisms associated with extreme precipitation, for the purpose of prediction of extreme precipitation and the identification of appropriate EPI and covariates. The response of extreme precipitation

TABLE 1 Summary of trend analysis of urban short-duration extreme precipitation in some regions

Country/region	Data	Methods	Key findings	References
Global scale	8,326 stations Annual maximum daily precipitation (1900–2009)	The Mann–Kendall nonparametric trend test method; non-stationary generalized extreme values models	The extreme precipitation of nearly two-thirds of stations worldwide exhibits increasing trend	Westra, Alexander, and Zwiers (2013)
Global scale	217 cities 24 hr rainfall extreme (1973–2012)	Mann–Kendall test; Theil–Sen's slope estimation method	Ten percent of annual maximum 24 hr rainfall in urban area shows a clear upward trend	Mishra et al. (2015)
China/Beijing-Tianjin-Hebei, Yangtze River delta	146 cities 24 hr rainfall data (1960–2014)	Define 6 extreme rainfall indices; ordinary least squares method; principal component analysis	Extreme precipitation in Beijing-Tianjin-Hebei shows a downward trend, while for Yangtze River delta an upward trend is confirmed	Zhou, Bai, and Yang (2017)
China/Shanghai	11 stations 1 hr rainfall data (1916–2014)	Linear tendency estimation method; Ensemble empirical mode decomposition; Mann–Kendall test	The annual maximum 1 hr rainfall shows a significant upward trend	Liang and Ding (2017)
China/Hong Kong	Hong Kong station 1 hr rainfall data (1885–1939 and 1947–2010)	Design rainfall based on EVT and generalized Pareto distribution; Sliding window	The 1 hr rainfall extremes in the urban area of Hong Kong has shown a clear increasing trend	Lenderink et al. (2011)
China/South	2,420 stations 1 hr precipitation (1982–2012)	Student's <i>t</i> test Mann–Kendall test	There is a clear increasing trend of hourly precipitation extremes in South China	Fu et al. (2016)
Indonesia/Jakarta	Jakarta station 1 hr rainfall data (1866–1950 and 1959–2010)	Linear regression 5-year moving window	No significant trend in the 5-year moving average of the annual maximum 1 hr rainfall is found	Siswanto, Van Oldenborgh, Der Schrier, Jilderda, and Van Den Hurk (2016)
Japan Nationwide	92 stations Rainfall with duration 10 min, 1 hr, 24 hr (1951–2010)	Linear regression Annual maxima and 95th percentile	Ten minutes rainfall extremes show the most significant upward trend	Fujibe (2013)
Peninsular Malaysia	25 stations 1 hr rainfall data (1975–2010)	Linear regression	One hour precipitation extremes show an upward trend	Syafrina, Zalina, and Juneng (2015)
India/Hyderabad	1 hr rainfall data (1971–2013)	Define four extreme rainfall indices; Linear regression; <i>F</i> -test	During the monsoon months, the frequency and intensity of 4 hr rainfall have increased	Agilan and Umamahesh (2015)
India/Northwest	33 cities 24 hr rainfall data (1971–2005)	Mann–Kendall test Theil–Sen's slope estimation method	Annual maximum 24 hr rainfall in 18% of cities shows a clear trend	Pingale, Khare, Jat, and Adamowski (2014)
Australia/Sydney	Sydney station Rainfall data with duration between 6 min and 72 hr (1921–2005)	Comparison of the 10-year moving average and the long-term series average	Changes in rainfall frequency and magnitude are closely related to season, duration, and rainfall threshold	Jakob et al. (2011)

TABLE 1 (Continued)

Country/region	Data	Methods	Key findings	References
Belgium/Uccle, Brussels	Uccle station 10 min precipitation extremes 107-year time series	Frequency analysis for moving window with 5 and 15 years	10 min precipitation extremes increase significantly	Ntegeka and Willems (2008)
Czech Republic	17 stations 30 min rainfall data (1961–2011)	Theil-Sen's slope estimation method	Precipitation extremes of most stations are increasing	Hanel, Pavlaskova, and Kysely (2016)
Denmark Nationwide	66 stations Rainfall data with duration between 1 min and 48 hr (1979–2005)	Analyze the changes in the estimated IDF curves between 1979–1997 and 1979–2006	10-year design rainfall between 30 min and 3 hr increased by more than 15%; intensity of rainfall over 24 hr did not change significantly	Madsen, et al. (2009)
United Kingdom Nationwide	1,311 stations 1 hr rainfall data (1982–2011)	Least squares regression Mann–Kendall test	Average hourly rainfall intensity trend is significant, but the annual extreme rainfall has no significant trend	Blenkinsop and Fowler (2014)
United States Nationwide	More than 6,000 stations Hourly precipitation data (1950–2011)	Mann–Kendall test Pettitt test Nonstationary GEV model	Both hourly and daily rainfall extremes have significantly increased over the last six decades across the U.S.	Barbero et al. (2017)

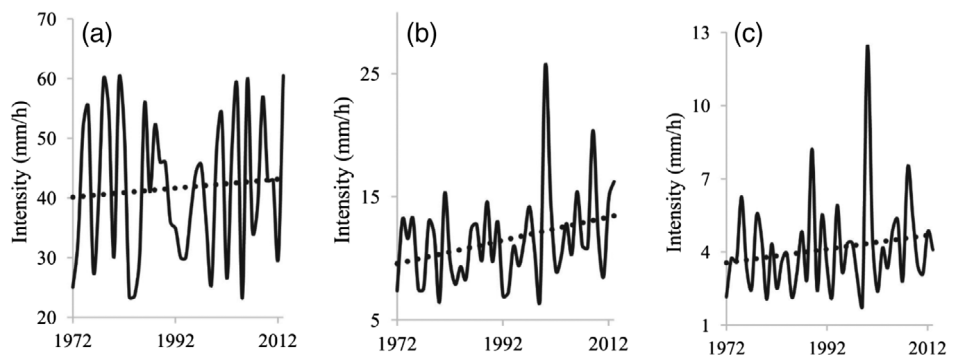


FIGURE 1 Variations in (a) 1 hr, (b) 6 hr, and (c) 24 hr duration annual maximum rainfall of the Hyderabad city and linear best fit of the variation (dashed lines; Agilan & Umamahesh, 2017)

to climate change is governed by two major physical mechanisms, namely the thermodynamic mechanisms and the dynamic mechanisms.

2.2.1 | Thermodynamic mechanisms

Thermodynamic mechanisms determine the relationship between water-holding capacity and temperature. According to the thermodynamic Clausius–Clapeyron (C–C) curves, rising temperature is anticipated to increase the water-holding capacity of air at a rate of approximately $7\text{ }^{\circ}\text{C}^{-1}$ (Fischer & Knutti, 2015). It is widely accepted that saturation water pressure (i.e., the water holding capacity) can be characterized by air temperature and pressure. Therefore, the precipitation–temperature scaling has served as a guideline in many studies for studying the changing properties of extreme precipitation. It should be noted that this simplistic view remains a subject of debate because an air mass containing more water does not indicate that this water is released. Many studies have been conducted worldwide to analyze the relationship between temperature and short-duration extreme precipitation. Nevertheless, it was found that the extreme precipitation can deviate from the C–C relationship in many regions. In the mid-latitude regions, changes in the intensity of sub-daily extreme precipitation can reach up to twice the C–C relationship (Lenderink et al., 2011; Westra et al., 2014). On the contrary, in some regions, evidence suggested that even decrease in the intensity of extreme precipitation with warming can happen (Lenderink & Fowler, 2017). This deficiency is due to the fact that air temperature cannot directly reflect humidity. Thus, Lenderink et al. (2011) explored the relationship between hourly extreme precipitation and dew point temperature, which directly corresponds to humidity, and found that the change of hourly extreme precipitation could be better explained by dew point temperature. However, it is difficult to distinguish the cause from effect since both precipitation and temperature could be affected by the impacts of atmospheric circulation (Lenderink et al., 2011; Westra et al., 2014). In addition, precipitation types and durations could modulate the precipitation–temperature scaling relationship (Berg & Haerter, 2013; Wasko, Sharma, & Johnson, 2015). Therefore, the changes in short-duration extreme precipitation could not be directly explained using the precipitation–temperature scaling method (Lenderink & Fowler, 2017). Precipitation–temperature scaling can only be considered as one possible guideline for interpreting those changes. In fact, rainfall occurrence not only depends on air temperature, but also water content, temperature and water content gradients, which can be regarded as the possibility of air masses to get humidity from evaporation over a water surface (sea) or evapotranspiration over a forested area. Besides, it also depends on the local pressure gradients and the possible rate of decrease in temperature of air masses.

2.2.2 | Dynamic mechanisms

The thermodynamic mechanisms are now generally well understood, while the theory of dynamic mechanisms associated with extreme precipitation has not been fully developed (O'Gorman, 2015). Dynamic mechanisms determine the occurrence of multiscale weather systems (e.g., extratropical cyclones, tropical plumes, and tropical cyclones), and their interactions drive the transport of atmospheric moisture and create the conditions (e.g., cyclonic conditions, convection) for rapid water condensation (Liu et al., 2020; Trenberth, 1999). To further reveal the dynamic mechanisms of

changes in extreme precipitation, Pfahl, O'Gorman, and Fischer (2017) employed the measure of condensation in updraft to diagnose the occurrence of extreme precipitation based on the simulation results of 22 global climate models (GCMs) from the Coupled Model Intercomparison Project Phase 5 (CMIP5). They decomposed the forced response of daily regional extreme rainfall in the simulations of climate-model into thermodynamic and dynamic contributions using a robust physical diagnostic and reproduced the daily extreme precipitation worldwide for the present climate. The simulations benefited from the physical formulation, which relies on both the atmospheric moisture and the vertical velocity of the air.

2.2.3 | Further the process understanding of extreme precipitation

Under changing environment, the physically-based diagnostic methods can provide feasible schemes for identifying the physical mechanisms associated with extreme precipitation. In fact, there are a large body of scientific literature providing analysis and simulation of extreme precipitation to better comprehend the underlying key processes controlling extreme precipitation at regional scale (Couto, Ducrocq, Salgado, & Costa, 2016; Ducrocq et al., 2016; Mure-Ravaud, Ishida, Kavvas, Yegorova, & Kanney, 2019; Mure-Ravaud, Kavvas, & Dib, 2019; Sauvage, Brossier, Bouin, & Ducrocq, 2020; Yang, Smith, Yang, Baeck, & Ni, 2019; Zhang et al., 2018). Among them, Ducrocq et al. (2016) highlighted the advances in process understanding of heavy precipitation in the Mediterranean in terms of initiation of deep convection, mesoscale convective systems dynamics and microphysics, and origin and transportation of water vapor. Sauvage et al. (2020) investigated the air-sea exchange mechanisms during a heavy precipitation in the Mediterranean, and found that the forecast of the heaviest precipitation could be modified when the realistic sea state was taken into account. Based on the Weather Research and Forecasting (WRF) model, Mure-Ravaud, Ishida, et al. (2019) reconstructed extreme precipitation and moisture transportation for six tropical cyclones affecting the eastern United States using the WRF numerical model, and found that horizontal moisture convergence played a key role in the generation of extreme precipitation in those tropical cyclones. However, the driving factors of the extreme rainfalls differ from one place to the other and can hardly be directly related to the outputs of GCMs. Zhang et al. (2018) quantitatively evaluated the contribution of urbanization to precipitation and flooding caused by hurricane Harvey in Houston using high-resolution WRF, and found that both urban flooding and total precipitation volumes can be exacerbated by urbanization. Because a feasible reason is the exacerbation of convection by local UHI, especially at the start of the rainfall events. Yang et al. (2019) analyzed the impacts of urban irrigation (i.e., irrigation for public greenspaces) on surface heat fluxes and precipitation in central Arizona using a high-resolution WRF model with or without an irrigation scheme. They found that urban irrigation had little impact on the average precipitation volume, but can significantly alter the spatial distribution of precipitation. In future, we should enhance the observation capabilities of extreme precipitation at finer temporal and spatial resolutions. More efforts would be needed to develop regional climate models or small-scale meteorological models, which can explicitly resolve convention and not convention conditions to further improve our physical and process understanding of urban short-duration extreme precipitation.

3 | COVARIATE-BASED NS IDF CURVES

3.1 | NS models

Under ST conditions, the intensities of extreme precipitation corresponding to various design return periods for different durations can be estimated. The annual maxima series for different durations (e.g., 15-min, 30-min, 1-hr, 2-hr, 6-hr, 12-hr, and 24-hr) are first fitted by a theoretical probability distribution, and then precipitation intensities corresponding to various design return periods (e.g., 2-, 5-r, 10-, 25-, 50-, and 100-years) are determined (Boukhalifa, Meddi, & Gaume, 2018; Gaume, 2018). Based on the extreme value theory (EVT), the generalized extreme value (GEV) distribution is often used to model the annual maxima, such as the annual maximum extreme precipitation (AMEP). For the AMEP z_t ($t = 1, \dots, n$), the cumulative distribution function (CDF) of stationary GEV (GEV-ST) model is given by

$$\begin{cases} G(z_t|\mu, \sigma, \epsilon) = \exp\left\{-[1 + \epsilon(z_t - \mu)/\sigma]^{-1/\epsilon}\right\}, & t = 1, \dots, n \\ 1 + \epsilon(z_t - \mu)/\sigma > 0 \end{cases} \quad (1)$$

where, $-\infty < \mu < \infty$, $\sigma > 0$, and $-\infty < \varepsilon < \infty$ are the location, scale, and shape parameters of the GEV-ST model, respectively. It should be noted that $\varepsilon \rightarrow 0$, $\varepsilon > 0$, and $\varepsilon < 0$ correspond to Gumbel, Fréchet, and Weibull distributions, respectively. Under ST conditions, the statistical parameters of GEV are time-invariant. However, under NS conditions, the statistical parameters of GEV model are time-dependent and can be modeled as a function of time or other physical covariates for capturing the changing properties of AMEP. The CDF of a fully nonstationary GEV (GEV-NS) model is defined as

$$\begin{cases} G_t(z_t|\mu_t, \sigma_t, \varepsilon_t) = \exp\left\{-[1 + \varepsilon_t(z_t - \mu_t)/\sigma_t]^{-1/\varepsilon_t}\right\}, t = 1, \dots, n \\ 1 + \varepsilon_t(z_t - \mu_t)/\sigma_t > 0 \end{cases} \quad (2)$$

where $G_t^{-1}(\cdot)$ denotes the time-varying CDF of the GEV-NS model. μ_t , σ_t , and ε_t are the time-varying location, scale, and shape parameters of the GEV-NS model, respectively, and t is the time index. Theoretically, all the three parameters can be modeled as function of time or other physical covariates. Under NS conditions, the parameters should be considered as time-dependent, which can be expressed as

$$\begin{cases} h(\mu_t) = \alpha_0 + \sum_{j=1}^m \alpha_j x_j^t \\ h(\sigma_t) = \beta_0 + \sum_{j=1}^m \beta_j x_j^t \\ h(\varepsilon_t) = \gamma_0 + \sum_{j=1}^m \gamma_j x_j^t \end{cases} \quad (3)$$

where $h(\cdot)$ is the link function, such as logarithm function. $\alpha = (\alpha_0, \dots, \alpha_m)$, $\beta = (\beta_0, \dots, \beta_m)$, and $\gamma = (\gamma_0, \dots, \gamma_m)$ are model parameters to describe the trends of μ_t , σ_t , and ε_t , respectively. x_j ($j = 1, \dots, m$) are the time-dependent covariates employed to explain the changing properties of extreme precipitation, and m is the number of used covariates.

Obviously, the number of estimated parameters of the GEV-NS model is larger than that of a ST model, and its model structure is more complex. Moreover, a question behind the choice of a NS model is the problem of uncertainties associated with statistical inference. There may be some trends in the observed extreme precipitation series, but these trends must be sufficiently significant to support the calibration of a more complex NS statistical model. Otherwise, the potential gain in accounting for the trend in the statistical model will be compensated by increased inference uncertainties, that is, uncertainties in the calibrated parameters of the statistical model and in the corresponding estimated quantile values (Yan et al., 2019). In other words, there is a trade-off, which is explicitly or implicitly considered, between model complexity and parameter estimation uncertainties. The trade-off between adequacy and accuracy of the model is at the core of the choice of NS models in statistics. Ideally, Bayesian statistical inference methods should be employed in modern statistical approaches to tackle this trade-off problem, since Bayesian statistical inference methods can provide a convenient way to fit distributions for precipitation frequency analysis, and information about the uncertainties in both distribution parameters and design values (Bertola, Viglione, & Blschl, 2019; Boukhefifa et al., 2018; Gaume, 2018; Viglione, Merz, Salinas, & Bloeschl, 2013). Boukhefifa et al. (2018) proposed a Bayesian approach for integrated estimation of IDF curves considering the linkage between IDF curves and properties of precipitation, such as simple scaling and multifractality, denoted by method M1. They comprehensively compared the proposed integrated approach, that is, M1, and the traditional approach in which probability distribution of precipitation was calibrated for each duration separately (method M0). It was found that the credibility intervals of design quantiles estimated using the M1 method were significantly lower compared with those estimated using the M0 method (Figure 2). Besides, the M1 method appeared to be robust for series with short record length.

3.2 | What are the best covariates for NS IDF curves?

To model the changing properties of NS extreme precipitation, the time-varying statistical parameters should be described as functions of covariates using the generalized linear model (GLM) for instance, or generalized additive model for location, scale, and shape parameters (GAMLSS) which is more powerful and flexible (Qu, Li, Yan, &

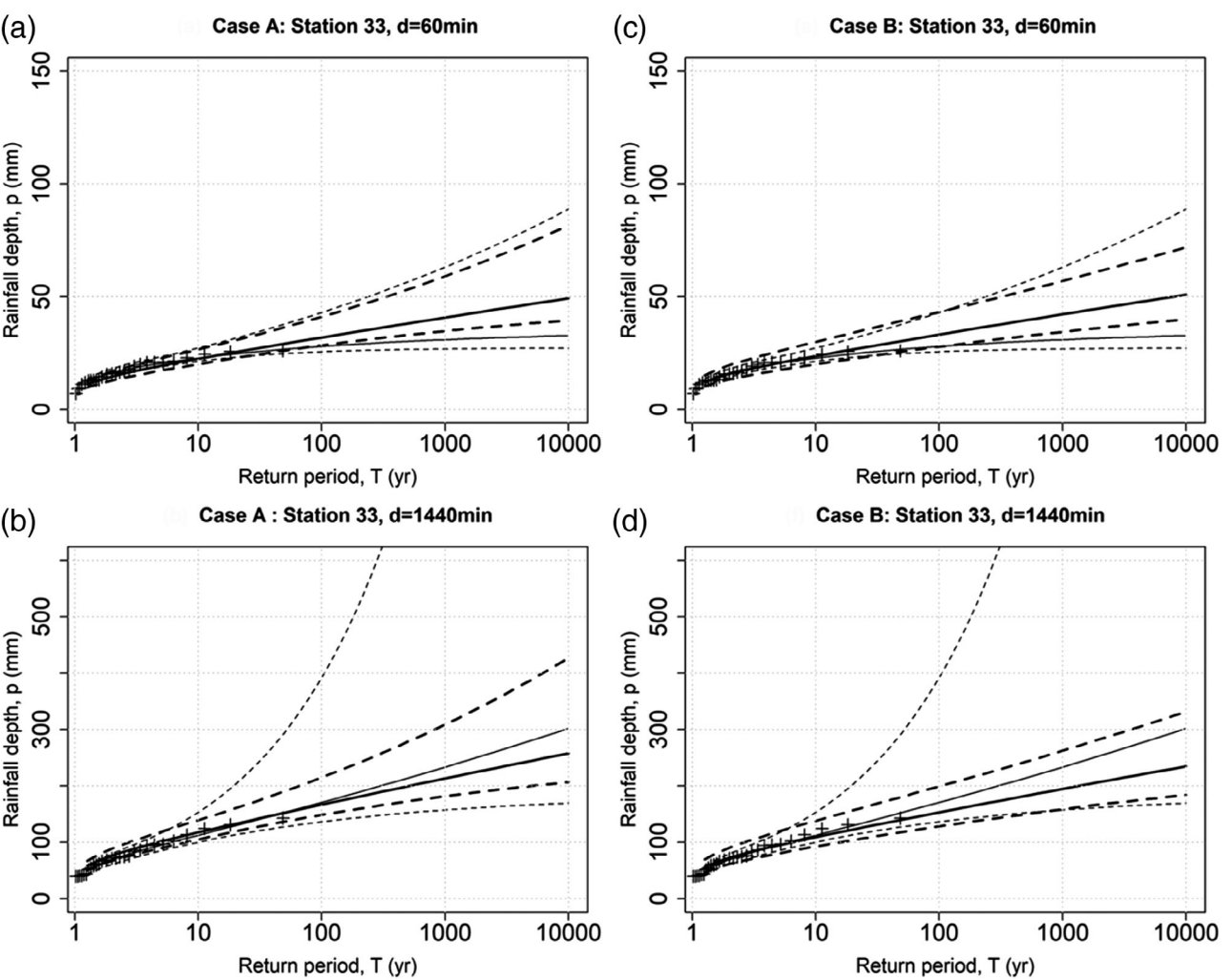


FIGURE 2 Rainfall depths annual maximum series fitted to a generalized extreme value distribution. (a,b) For the Case A (15 min–24 hr) and (c,d) for Case B (60 min–24 hr). Crosses for observed values. Thin lines: M0 model. Thick lines: M1 model. Dashed lines: 90% credibility intervals (Boukhaled et al., 2018)

Lu, 2020; Rigby & Stasinopoulos, 2005). Theoretically, while all the three statistical parameters of GEV-NS models can be described as time-varying parameters, the shape parameter in Equations (2) and (3) is sensitive and difficult to estimate (Cheng & Aghakouchak, 2014; Du et al., 2015; Um, Kim, Markus, & Wuebbles, 2017). Thus, the GEV-NS models generally considering the changing properties of location parameter μ_t and/or scale parameters σ_t in Equation (3) are widely used in practical applications. These simplified GEV-NS models can yield realistic design precipitation quantiles consistent with the probabilistic behavior of extreme precipitation (Cheng & Aghakouchak, 2014; Sarhadi & Soulis, 2017).

In the implementation of NS models, it is crucial to strengthen the physical meaning of the established statistical model, instead of doing a statistical exercise without paying much attention to the physical process of extreme precipitation (Yan et al., 2017). Moreover, the prediction of future evolution of the probability distribution of extreme precipitation is one of the most challenging issues in the estimation of NS design precipitation intensities, which strongly depends on the projections of covariates in future period. Therefore, it is essential to select appropriate covariates associated with extreme precipitation. In most recent studies, only time covariate was used to simulate nonstationarity of extreme precipitation. Cheng and Aghakouchak (2014) proposed a general framework for developing NS IDF curves using the GEV-NS model with time covariate for the demonstration purpose. Yan, Xiong, Guo, et al. (2017) argued that the covariates used for NS frequency analysis should satisfy two requirements: (i) able to describe the changing properties of extreme events and (ii) able to be reliably predicted in future period. From this perspective, mean temperature might be the best predicted variable provided by GCMs. Some studies (Agilan & Umamahesh, 2016; Agilan &

Umamahesh, 2017) comprehensively evaluated possible covariates associated with extreme precipitation, namely urbanization, temperature, global warming (The yearly observed Global Temperature Anomaly for the period of 1961–1990 mean was employed as an indicator of global warming), El Niño Southern Oscillation index (ENSO), Indian Ocean Dipole (IOD), and time (Figure 3). By employing the corrected Akaike Information Criterion (AICc) to identify the best GEV model with appropriate covariates, they found that local processes (e.g., urbanization and temperature) were the best covariates for local short-duration extreme precipitation, while global processes (e.g., global warming, ENSO, and IOD) were the best covariates for long-duration extreme precipitation (Figure 4). Besides, time covariate was not recommended for constructing NS IDF curves. Sarhadi and Soulis (2017) constructed the GEV-NS model using both time and Southern Oscillation Index (SOI) in deriving NS IDF curves of the Great Lakes area. Their results showed that, for most stations, the GEV model with both location and scale parameters varying with time was the best model, while the GEV model with SOI covariate was the next best model, indicating the influence of low frequency climate signals on the extreme precipitation in the Great Lakes area. Ouarda, Yousef, and Charron (2019) developed the GEV-NS and Gumbel models using time and climate indices, such as Atlantic Multi-decadal Oscillation (AMO) and Western Hemisphere Warm Pool (WHWP) for the stations in Canada, and SOI and Pacific Decadal Oscillation (PDO) for the stations in United States. They found that time and AMO were the best covariates for the two selected stations in Canada, and SOI and PDO were the best covariates for the station located in United States.

3.3 | NS design methods for estimating precipitation intensities

The statistical parameters of GEV-NS models are described as a function of time or other physical covariates. Thus, how to estimate the NS design precipitation with a prescribed return period under NS condition is one of the core questions (Acero et al., 2017; Acero, Parey, García, & Dacunha-Castelle, 2018; Jiang, Xiong, Yan, Dong, & Xu, 2019; Salas & Obeysekera, 2014; Yan, Xiong, Guo, et al., 2017). According to the design concepts under ST condition, the annual design precipitation associated with a given return period varies over time. Obviously, this kind of time-varying annual design precipitation would be impractical for urban infrastructure design and storm water management under changing environment, since the relationship between design criterion and design value is no longer one-to-one. As displayed

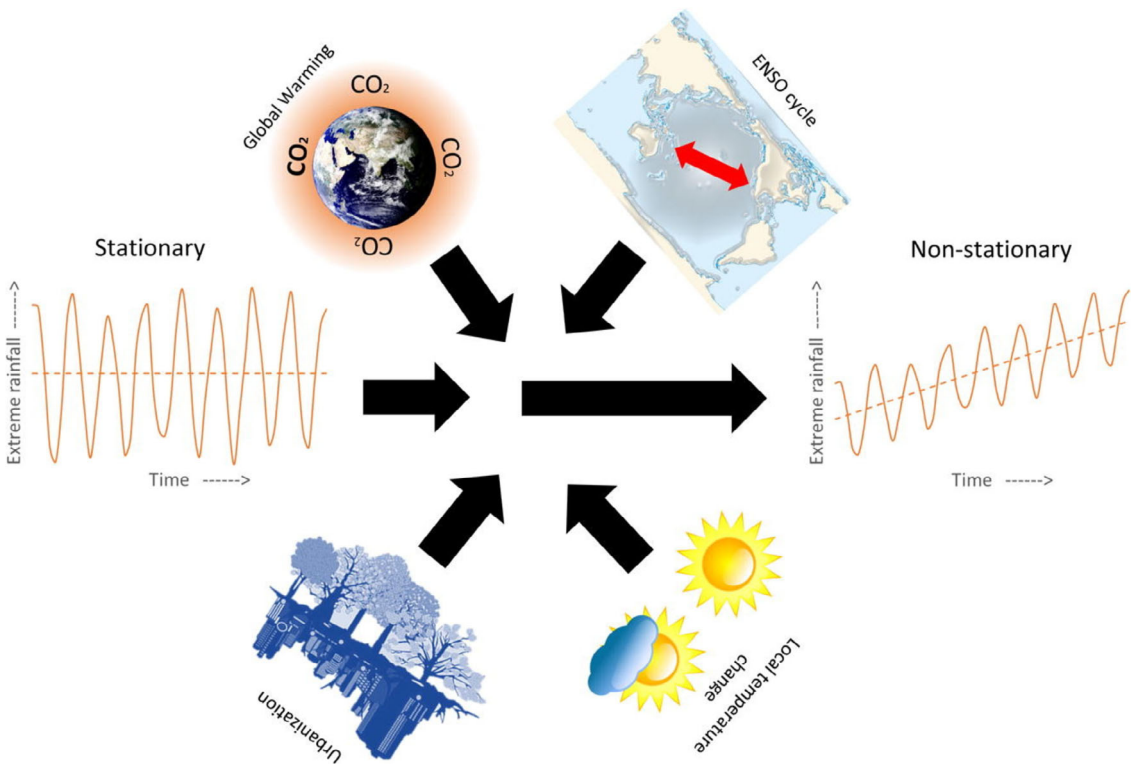


FIGURE 3 The global process and local process that are supposed to destroy the stationary assumption (Agilan & Umamahesh, 2015)

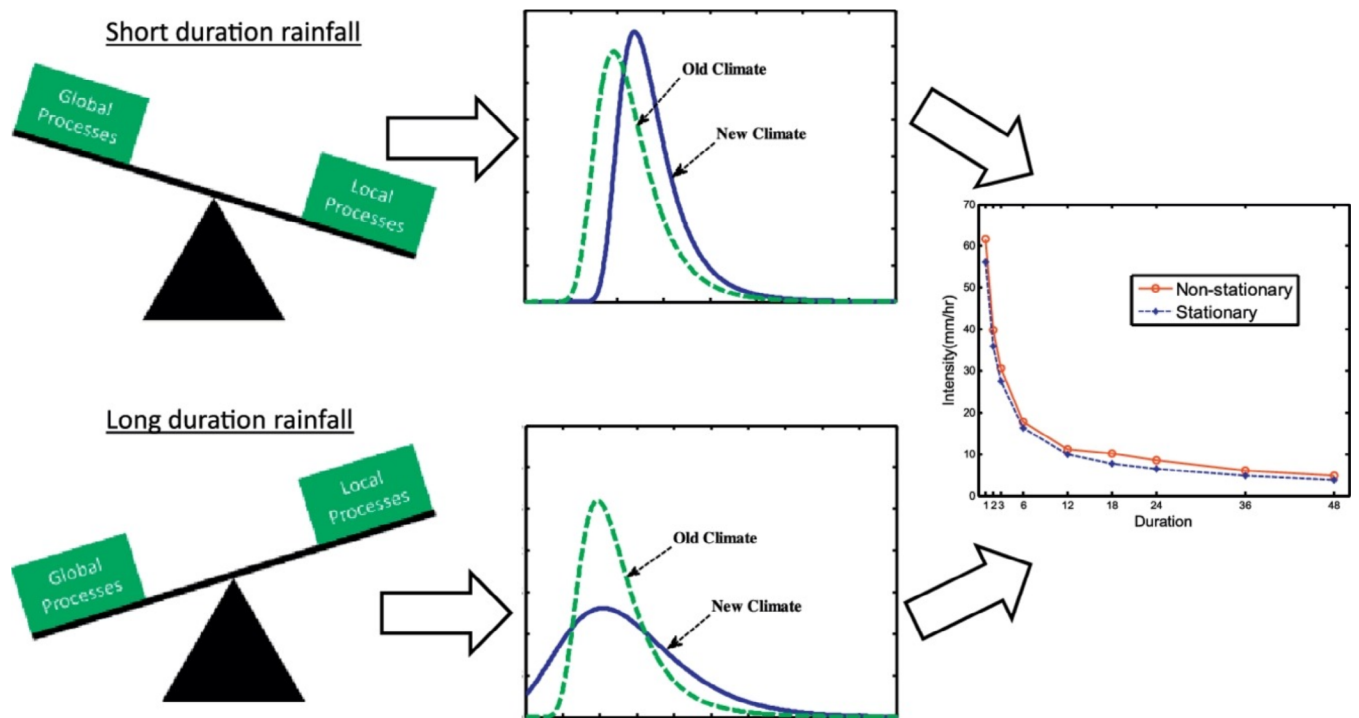


FIGURE 4 Schematic diagram showing the relative contribution of the global process and local process to long-duration and short-duration rainfall, respectively (Agilan & Umamahesh, 2017)

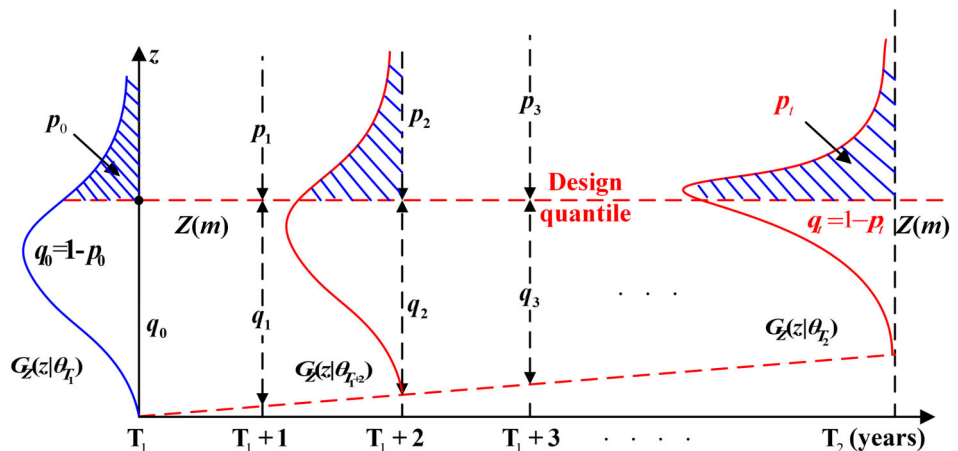


FIGURE 5 Schematic diagram depicting the evolution of probability distributions of extreme events from T_1 year to T_2 year. p_i is the time-varying exceedance probability in case of an increase of the intense rainfall frequencies or intensities

In Figure 5, for a given design quantile, the exceedance probabilities p_0 can change with time. It is less feasible to adapt our infrastructures such as drainage system year by year. Thus, the design value should be defined for a given time horizon. The design value is expected to reach the correct design target at the end of the considered period or on average over the considered period.

In recent years, several NS design methods have been proposed to tackle the problem of design precipitation estimation under NS condition (Acero et al., 2018; Cheng & Aghakouchak, 2014; Hu et al., 2018; Olsen, Lambert, & Haimes, 1998; Parey, Hoang, & Dacunha-Castelle, 2010; Parey, Malek, Laurent, & Dacunha-Castelle, 2007; Rootzén & Katz, 2013; Salas & Obeysekera, 2014; Yan, Xiong, Guo, et al., 2017). Volpi (2019) provided a detailed discussion about the concept of return period and the related risk of failure using a general mathematical framework, and extended the concept of return period to NS conditions. That study emphasized that fitting a NS model to series with significant trend

requires additional efforts in regard to the ST, independent and traditional yet not trivial cases. It is important to understand that there is no unique or correct definition of design values for NS situation. It depends on the need of the user: obtain an average design value (i.e., an expected exceedance values) over the design period or ensure that the design still satisfy the design target at the end of the period.

Several studies have been conducted to obtain design value, which is expected to reach the correct design target on average over the prescribed period. Initially, Cheng and Aghakouchak (2014) determined the time-invariant location parameter of GEV model using the 95th percentile of the varying annual location parameters in observation period, and obtained a unique value over the observation period. Then the ST design concepts can be used to derive design precipitation corresponding to a specified return period. Agilan and Umamahesh (2016, 2017) also calculated distribution parameters using the 95th percentile of the location parameters and scale parameters in the historical period to estimate the so-called effective return level. They found that compared with the IDF curves derived from the NS models, those estimated from ST models underestimated the precipitation intensities of all durations and for all return periods (Figure 6). Based on two different interpretations of return period under stationarity, the expected waiting time (EWT; Cooley, 2013; Olsen et al., 1998) and expected number of exceedances (ENE) methods were further modified to account for nonstationarity (Parey et al., 2007, 2010). Volpi (2019) provided an excellent review concerning the definition of return period in both ST and NS conditions. Cooley (2013) presented the mathematical expressions of ENE and EWT methods under both ST and NS contexts. By comparing the difference between EWT and ENE methods in calculating NS design flood, Hu et al. (2017) reported that, in the case of a decreasing trend, the design values estimated using the EWT method were smaller than those estimated using the ENE method. While in the case of increasing trend, design values estimated using the EWT were larger than those estimated using the ENE method. Yan et al. (2020) explored the applicability of the EWT method in NS flood design, and suggested that the extrapolation time of the EWT method for stations with upward trends was significantly smaller than that of stations with downward trends.

Under changing environment, the design life of a project should be considered in the NS design because the risk of failure is different for different future periods. In recent years, researchers have developed several well-designed NS design methods considering the design lifespan of projects. The concept of design life level (DLL) was proposed by Rootzén and Katz (2013) to communicate the reliability $RE_{T_1-T_2}^{ns}$ (ns denoting nonstationary) of a project over its design lifespan starting from T_1 to T_2 . For a given reliability $RE_{T_1-T_2}^{ns}$, the design value $z_{T_1-T_2}^{DLL}$ can be estimated using $RE_{T_1-T_2}^{ns} = \prod_{t=T_1}^{T_2} G_Z(z_{T_1-T_2}^{DLL} | \theta_t)$, in which G is the cumulative distribution function. However, how to determine the reasonable value of reliability that urban infrastructures will experience over the design lifespan may be a challenging

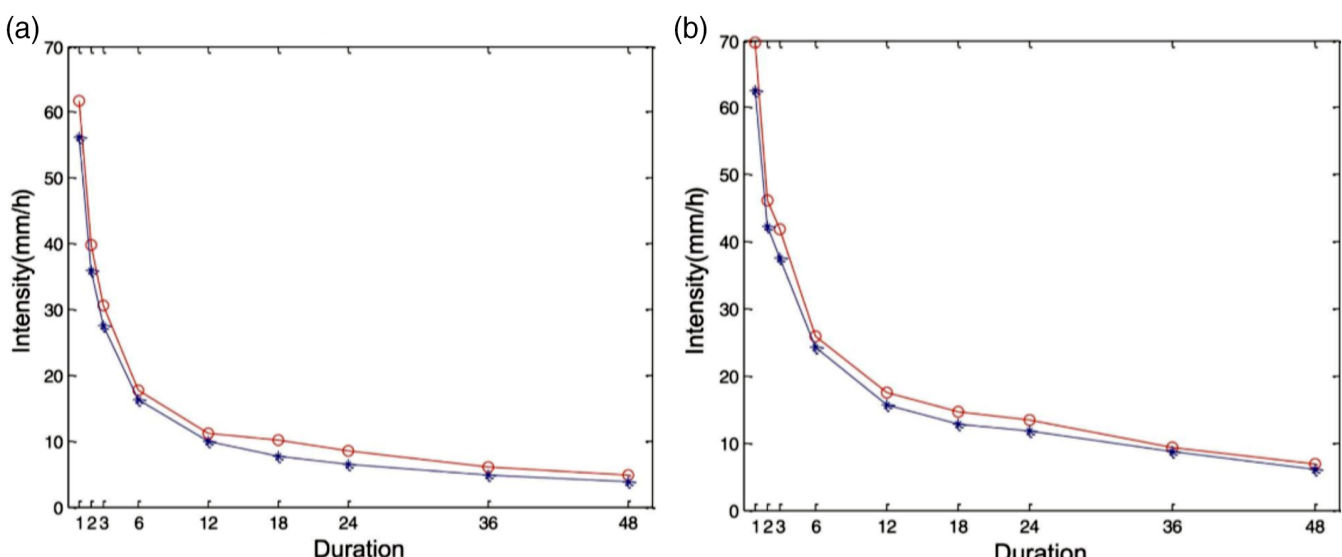
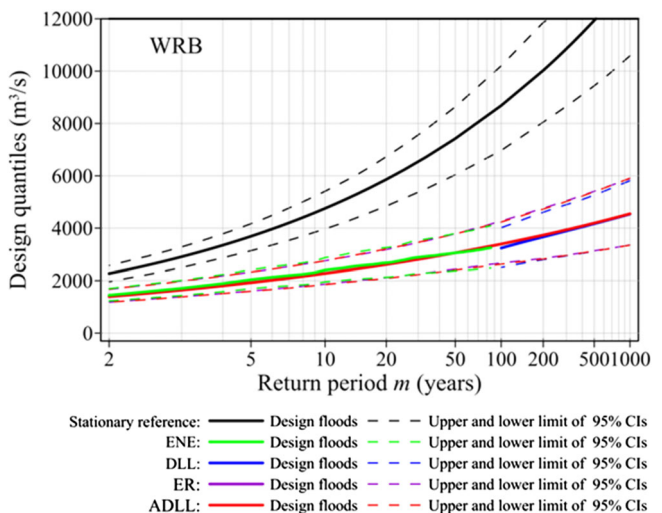


FIGURE 6 Non-stationary intensity-duration curves of Hyderabad city for (a) 10 year and (b) 100 year return periods (Agilan & Umamahesh, 2017)

FIGURE 7 Return level diagrams for WRB (a) using different design approaches (ENE, DLL, ER, and ADLL) with 95% bootstrapped confidence intervals under the covariate scenario 2. The covariate scenario 2 refers to the projected precipitation under RCP4.5 and population. The solid lines are the design floods while the dashed lines are the upper and lower limits of the 95% confidence intervals



work, for the reason that engineers and decision makers are more familiar with the concept of return period, which has served as basis of engineering design for decades. Therefore, Hu et al. (2018) proposed the concept of equivalent reliability (ER). In this method, the reliability over a project's design lifespan under NS conditions, that is, $RE_{T_1-T_2}^{ns}$, is assumed to be identical to the reliability under ST conditions $RE_{T_1-T_2}^s$, which is given by $RE_{T_1-T_2}^s = (1 - 1/m)^{T_2 - T_1 + 1}$ corresponding to return period m . It should be mentioned that in the ER method, we first estimate $RE_{T_1-T_2}^s$ for a given return period m in a ST situation, and then calculate the corresponding design value over the design period in a NS situation. Yan, Xiong, Guo, et al. (2017) proposed another NS design method, that is, average design life level (ADLL), to estimate the design value $z_{T_1-T_2}^{ADLL}(m)$ and argued that the annual average reliability over a project's design lifespan under nonstationarity, which is $\sum_{t=T_1}^{T_2} G_Z(z_{T_1-T_2}^{ADLL}(m)|\theta_t)/(T_2 - T_1 + 1)$, should be equal to that of yearly reliability $1 - 1/m$ corresponding to the return period m . To investigate the performance of the above NS hydrological design methods, Yan, Xiong, Guo, et al. (2017) compared the design results estimated using the ENE, DLL, ER, and ADLL methods. They found that the ENE, ER, and ADLL methods can yield similar design results using physically-based covariates (Figure 7). A clear definition of all the mentioned design methods can be found in the Section 2.1 provided by Yan, Xiong, Guo, et al. (2017).

4 | CLIMATE-MODEL-BASED IDF CURVES

4.1 | Projections of future short-duration precipitation

Different from the projecting future IDF curves using NS models, evaluating the potential changes in IDF curves using simulated projections of climate model is a physically-based avenue. However, the temporal and spatial resolutions of GCM outputs are still too coarse to directly assess future changes of sub-daily precipitation, despite the progress made by GCMs participated in CMIP5. Therefore, downscaling and bias correction of outputs from GCMs or Regional Circulation Models (RCMs) to the desired spatial (i.e., spatial downscaling) and temporal (i.e., temporal downscaling) resolutions for assessing changes in urban short-duration extreme precipitation are necessary, and are becoming one of the demanding topics in recent years (Colmet-Daage et al., 2018; Schiemann et al., 2018; Willems, ArnbjergNielsen, Olsson, & Nguyen, 2012). Researchers have developed several approaches to generate future short-duration precipitation and update IDF curves with a range of complexities and underlying assumptions. These methods can be categorized into two major groups: (i) statistical downscaling methods (Hassanzadeh, Nazemi, Adamowski, Nguyen, & Van-Nguyen, 2019; Li, Johnson, Evans, & Sharma, 2017; Pastén-Zapata, Jones, Moggridge, & Widmann, 2020; Pui, Sharma, Mehrotra, Sivakumar, & Jeremiah, 2012) and (ii) dynamic downscaling models with high spatial and temporal

resolutions, for example, RCMs and Convention-permitting models (CPMs; Ban, Schmidli, & Schär, 2015; Liu et al., 2017; Prein et al., 2015, 2017; Zittis, Bruggeman, Camera, Hadjinicolaou, & Lelieveld, 2017).

4.1.1 | Statistical downscaling methods

Statistical downscaling methods are the most commonly used methods in projecting future sub-daily precipitation. They are relatively easy to understand and require less computational efforts than dynamic downscaling methods. Srivastav, Schardong, and Simonovic (2014) reviewed the existing statistical downscaling methods and categorized them into three groups:

- Delta change method. This method is usually used to transfer the signal of climate change from climate models to observations. The change factors (CFs) of GCM/RCM outputs between the baseline period and future periods are applied to manipulate the observed historical precipitation with different durations (Hosseinzadehtalaei, Tabari, & Willems, 2018; Mailhot, Duchesne, Caya, & Talbot, 2007; Semadeni-Davies, Hernebring, Svensson, & Gustafsson, 2008; Zahmatkesh, Karamouz, Goharian, & Burian, 2015). Taking the additive delta change method as an example, the mean values of GCM baseline (GCM_b) and future period (GCM_f) are used to calculate the additive (CF_{add}) CFs using $CF_{add} = GCM_f - GCM_b$. Then, the local scaled future precipitation $P_{add,f}$ can be obtained by applying CF_{add} to the local observed precipitation P_{ob} via $P_{add,f} = P_{ob} + CF_{add}$. A multiplicative delta change method is similar to an additive delta change method except that the ratio, rather than arithmetic difference, between the future and baseline periods of GCM/RCM outputs is calculated, and then the local future precipitation can be obtained by multiplying the CF to the local observed precipitation. More information can be found in Anandhi et al. (2011).
- Bias correction methods. In this method, differences between GCM/RCM simulation and observed precipitation for the historical period are first estimated, and then used to perturb GCM/RCM outputs in future periods (Hassanzadeh et al., 2014, 2019; Ngai, Tangang, & Juneng, 2017; Pastén-Zapata et al., 2020). Li et al. (2017) briefly described the two major bias correction options, namely the option to correct the total precipitation distribution and the option to correct the AM precipitation series.
- Downscaling-disaggregation methods. In this method, spatial downscaling and bias correction for GCM/RCM outputs are applied to generate future daily or monthly precipitation. Next, temporal disaggregation models are employed to disaggregate future precipitation from daily to sub-daily scales (Li et al., 2017; Mirhosseini, Srivastava, & Stefanova, 2013; Nguyen, Nguyen, & Cung, 2007; Pui et al., 2012). Li et al. (2017) and Pui et al. (2012) reviewed and compared different downscaling-disaggregation methods.

A good example of generating future sub-daily precipitation using statistical approach can be found in Agilan and Umamahesh (2016). In that study, future sub-daily precipitation was generated using the delta change method and KNN weather generator. More specifically, 2015–2056 and 2057–2098 were considered as two future periods, while 1972–2005 was considered as historical period. For each future period, the CF was calculated using the observations and the outputs of 23 GCMs. Besides, the intermodal uncertainties were tackled using the Reliability Ensemble Average method by assigning weighting coefficients to both historical and future periods. The CFs for the period 2015–2056 calculated using the Reliability Ensemble Average technique are presented in Figure 8. Then, the KNN weather generator method was applied to generate the future long-term plausible precipitation data. More technical details about the employed KNN weather generator method can be found in Sharif and Burn (2007) and Agilan and Umamahesh (2016). The aforementioned methods differ from each other in the way they simulate the relationship between GCM/RCM outputs and observed daily or sub-daily precipitation for the baseline period and how they utilize the changes between GCM/RCM simulated precipitation for the historical and future periods (Lima, Kwon, & Kim, 2016). The advantages and disadvantages of some above methods have been discussed by researchers (Lehmann, Phatak, Stephenson, & Lau, 2016; Lima et al., 2016; Pui et al., 2012; Srivastav et al., 2014). As emphasized by Lima et al. (2016), there is no well-accepted approach to obtain future precipitation and evaluate changes in IDF curves. The choice of different approaches is likely driven by personal expertise, method complexity, and desired temporal and spatial scales. All methods are based on the hypothesis that the transfer function between GCM outputs and measured rainfalls that is calibrated in the present period will remain unchanged in the future.

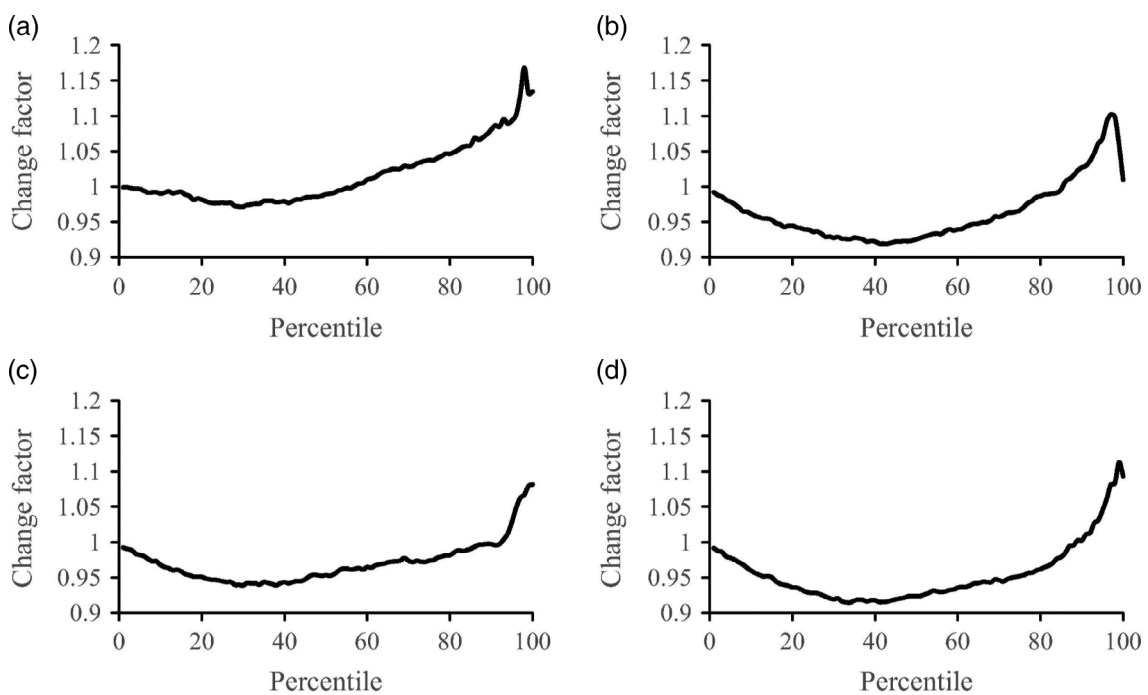


FIGURE 8 2015–2056 reliability ensemble average technique based change factors for (a) RCP 2.6, (b) RCP 4.5, (c) RCP 6.0, and (d) RCP 8.5 scenario

4.1.2 | Dynamic downscaling models with high spatial and temporal resolutions

Researchers have also developed more powerful climate models to better understand the physical process of extreme precipitation. For instance, the higher-resolution RCMs with 10–50 km spatial resolution are capable of improving the representation of daily extreme precipitation compared with GCMs. Moreover, researchers have reported that this kind of RCM with 10–50 km spatial resolution can better reproduce the observed sub-daily precipitation and capture the spatial structure of sub-daily precipitation extremes (Evans & Westra, 2012; Lenderink & Van Meijgaard, 2008; Tripathi & Dominguez, 2013; Westra et al., 2014). However, RCMs are still insufficient to reproduce the observed local sub-daily precipitation and represent the spatial characteristics of extreme short-duration precipitation, particularly when the required resolution is less than 10 km (Jiang, Gautam, Zhu, & Yu, 2013; Prein et al., 2015; Westra et al., 2014; Zhang, Zwiers, Li, Wan, & Cannon, 2017).

Currently, the development of CPMs with spatial resolution less than about 4 km is a popular topic in the field of numerical prediction. CPMs can sufficiently simulate the diurnal cycle of convective precipitation, the spatial structure of precipitation, and reproduce the intensities of extra-large extreme precipitation (Fosser, Kendon, Stephenson, & Tucker, 2020; Langhans, Schmidli, Fuhrer, Bieri, & Schar, 2013; Lind et al., 2020; Manola, van den Hurk, De Moel, & Aerts, 2018; Prein et al., 2017; Westra et al., 2014). Most of the current applications of CPMs are limited to a single season, because it would be too costly to perform long-term climate change simulations (Westra et al., 2014). They differ from GCMs/RCMs which use the convection parameterization schemes to account for the influence of convection over the model grid scale (sources of errors and uncertainties), the improvements of CPMs in projecting future short-duration extreme precipitation are attributed to their explicit solving of deep convection and better representation of local high-resolution orography and variations of surface fields (Clark, Roberts, Lean, Ballard, & Charlton-Perez, 2016; Liu et al., 2017; Westra et al., 2014; Zittis et al., 2017). Generally, CPMs can represent the spatial and temporal characteristics of the observed hourly extreme precipitation given correct boundary conditions, thus providing effective tools for analyzing the changes in future short-duration extreme precipitation. Despite the advances of CPMs in recent years, it remains questionable whether CPMs can adequately represent the spatial and temporal characteristics of observed rainfall, particularly for the long-term climate change simulations. For example, misallocation of the intense rainfall cells remains frequent, the role of some triggering factors is exacerbated and some subtle features due for instance to the re-evaporation of the

produced rainfall at the start of the events are difficult to capture. CPMs are becoming one of the powerful tools to help understanding the peculiarities of single rainfall event and analyzing the changes in future short-duration extreme precipitation. Nevertheless, they remain far from perfect and they need correct boundary conditions, thus requiring more research efforts.

4.2 | Derivation of future IDF curves

Once the future short-duration extreme precipitation is projected, the distribution of extreme precipitation with various durations can be determined for future period based on the statistical inference methods presented previously, and then the IDF curves and their related changes can easily be evaluated. Agilan and Umamahesh (2016) constructed future IDF curves for two future periods by using the GEV distribution to fit the future AM precipitation with different durations, which is extracted from the generated future long-term precipitation as mentioned in Section 4.1.1. Besides, the parameters of the GEV distribution were estimated using the maximum likelihood method. Apart from the GEV distribution, researchers have also explored other distributions for building IDF curves. Lima et al. (2016) proposed using a Bayesian beta model, which integrates a four-parameter beta distribution and Bayesian inference to derive IDF curves in South Korea based on GCM outputs for future climate. They found that the fitting qualities of the proposed Bayesian beta model are similar to the conventional GEV models, and the Bayesian beta model can be applied to disaggregate the future 24-hr precipitation to finer scales to facilitate the impact analysis of future changes to the current IDF curves. Ragno et al. (2018) developed NS models for bias corrected historical and multi-model projected extreme precipitation, and estimated IDF curves and the associated uncertainties using Bayesian inference framework, which is based on Bayesian inference and Differential Evolution Markov Chain. They indicated that the intensity is expected to increase by 20%, while the occurrence of extreme precipitation, that is, 90th quantile of the simulated 1 day extreme precipitation intensity, is twice as frequent as historical period for densely-populated regions in United States.

In addition to conducting frequency analysis directly on the projected future extreme precipitation with different durations, alternatively, future IDF curves can also be derived using delta change method based on projections of climate models. Hosseinzadehtalaei et al. (2018) first conducted frequency analysis for POT extreme precipitation statistics of both historical and future simulations in EURO-CORDEX project (an ensemble of 88 RCMs) using a two-component exponential distribution. IDF curves for the simulations of the EURO-CORDEX RCMs for 1-month, 1-year, and 10-year return periods were developed based on POT extreme value statistics and the fitted two-component exponential distribution. After that, they calculated the CFs of precipitation intensities for different return periods and durations, and applied these CFs on IDF statistics of observed extreme precipitation to generate IDF statistics for future period.

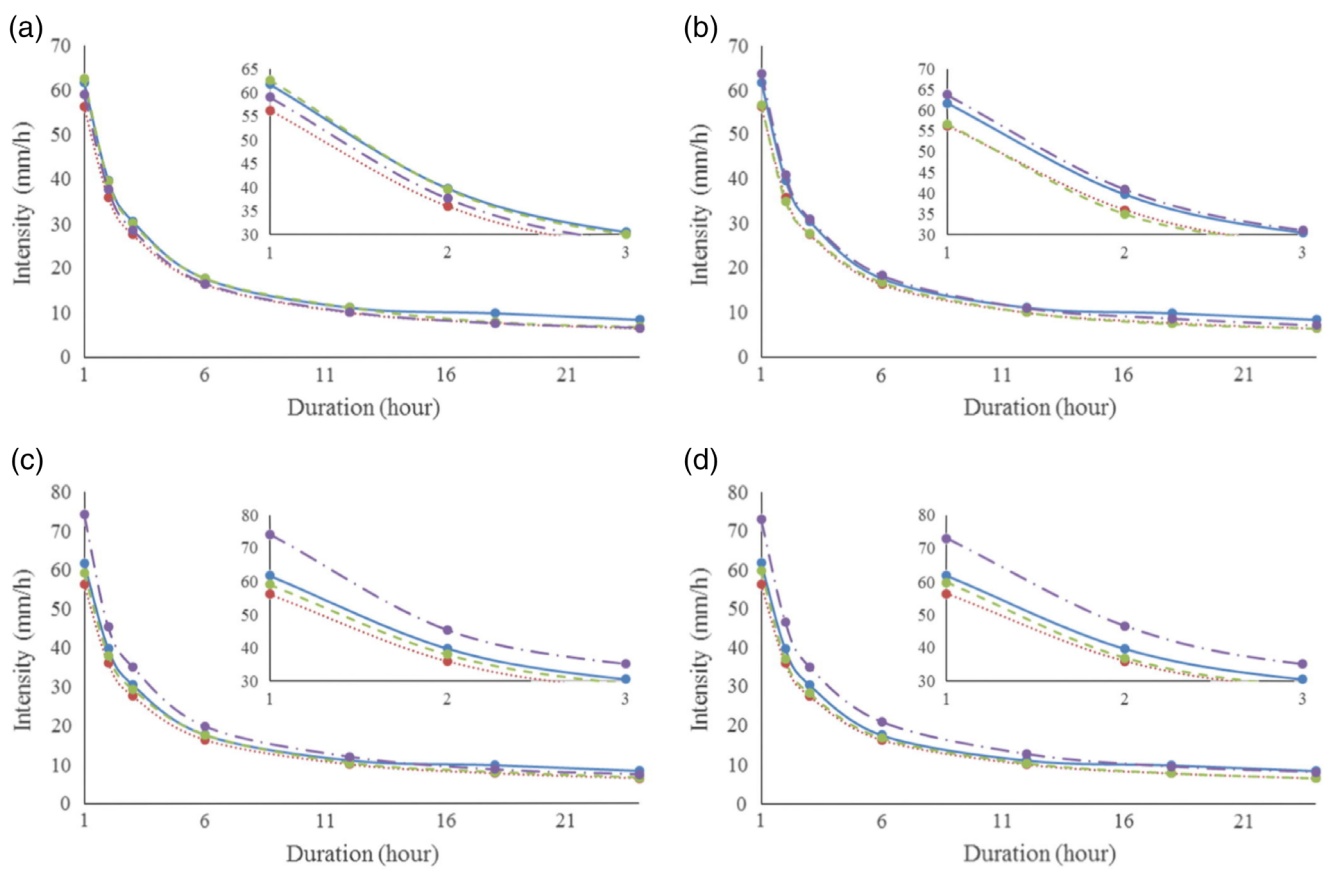
5 | SUMMARY

Under changing environment, the intensity and frequency of short-duration extreme precipitation are anticipated to increase for future climate in many places. This casts doubt on the ST assumption in urban infrastructure design and storm water management. Thus, the IDF curves should be updated to account for future changes in extreme precipitation. This study reviewed the changes in urban extreme precipitation and physical mechanisms. In particular, we tracked the current progresses in methods for updating IDF curves for future climate, namely the covariate-based NS IDF curves and climate-model-based IDF curves. The covariate-based NS models provide an avenue to predict future IDF curves based on observed and reliable sub-daily extreme precipitation. However, there is no well-accepted and non-controversial NS modeling approach. Meanwhile, the debates mainly focus on the predictive capabilities of NS model and the trade-off between uncertainties and model complexity. Reliable NS modeling requires attribution analysis to identify the physical causes of nonstationarity (Montanari & Koutsoyiannis, 2014; Serinaldi & Kilsby, 2015). Typically, the relationship between statistical parameters and covariates are assumed to be unchanged when projecting the distributions of future extremes, which may be unreasonable (Luke, Vrugt, AghaKouchak, Matthew, & Sanders, 2017; Ragno et al., 2018; Serinaldi & Kilsby, 2015). The climate-model-based methods highly rely on the projections of local high-resolution extreme precipitation, which contains some uncertainties, despite the improvements made in recent years, particularly for urban areas. Either the covariate-based NS IDF curves or the climate-model-based IDF curves have their own limitations, thus, further studies would be required to understand how to take advantage of both methods.

6 | DISCUSSION

There are limited studies comparing the differences and performances of these two methods. For example, Agilan and Umamahesh (2016) first developed the IDF curves based on 24 GCMs' simulated precipitation and K nearest neighbor weather generator based downscaling method, and the IDF curves derived using NS models with best physical covariates (i.e., urbanization, temperature, global warming, ENSO, and IOD), separately for the Hyderabad city, India. Then they compared the design precipitation with return periods of 2, 5, 10, and 25 years estimated using these two kinds of IDF curves. The design values of covariate-based NS IDF curves are considered as reasonable if they are greater than those estimated by climate-model-based IDF curves, indicating their ability to capture or encompass the future climate change signals. As illustrated in Figure 9, IDF curves derived from the covariate-based NS models lead to larger design values than those derived using 2015–2056 future rainfall of all RCP scenarios. These indicate that the covariate-based NS IDF curves are reasonable and able to capture the signal of climate change for at least future 50 years for the study area (Figure 9). From another perspective, Ragno et al. (2018) argued that one drawback of covariate-based NS IDF curves is the dependence of solely observed precipitation records for NS modeling, with an assumption that extrapolates the observed trends to the future periods, while GCMs outputs can offer plausible scenarios for future climate and can be incorporated for deriving future IDF curves. So, they tried to utilize both covariate-based and climate-model-based methods by developing NS models for future projected precipitation. Particularly, in their study, multiple GCMs outputs were processed using the NS extreme value analysis method proposed by Cheng and Aghakouchak (2014) to derive multi-model NS IDF curves.

Despite the increased emphasis on updating current IDF curves, there is still no well-accepted and noncontroversy methodology for updating IDF curves. In fact, there is not even agreement on the need for updating IDF curves. Ganguli and Coulibaly (2017) compared the current stationarity-based IDF curves with the covariate-based NS IDF



—●— Observed_Non-stationary ······ Observed_Stationary -·○- REA_GCM_2015-2056 -·●- REA_GCM_2057-2098

FIGURE 9 Ten-year return period stationary, nonstationary and future intensity–duration curves of (a) RCP 2.6, (b) RCP 4.5, (c) RCP 6.0, and (d) RCP 8.5 scenario

curves, and suggested no significant differences for short return period, which is commonly used in urban infrastructure design. Therefore, the signal of nonstationarity does not automatically imply the requirement of updating IDF curves for urban design considerations. However, some efforts have been made by governments to highlight the need for updating IDF design guidelines. For example, guidelines for Canadian water resources practitioners (CSA, 2010) emphasizes the necessity to update IDF curves more frequently than previous periods to account for the possible increase in intensity and frequency of extreme precipitation in Canada.

7 | FUTURE CHALLENGES

Regarding urban design strategies, it is crucial to revisit the current IDF design guidelines and assess the possible impacts of future climate. Thus, collaborative and interdisciplinary research efforts involving with engineers, climate scientists and decision makers are required for updating the design strategies for IDF curves (Cheng & Aghakouchak, 2014; Ganguli & Coulibaly, 2017; Ragno et al., 2018). In the following section, we put forward some future research possibilities and challenges in updating IDF curves under changing environment, which should enable us to better understanding of changing properties of short-duration extreme precipitation and assist urban infrastructure design.

1. High-quality subdaily extreme precipitation is essential for impacts analysis of climate change and updating IDF curves for future climate. However, the record lengths of available subdaily precipitation are limited and their qualities are not always satisfactory. Moreover, free access to high-quality sub-daily precipitation records is uncommon in many countries. Currently, remotely sensed satellite precipitation products and ground-based radar products provide new avenues to obtain sub-daily precipitation data (Chen et al., 2020). Nonetheless, their measurement errors have become a major constrain on studying precipitation extremes. Pluviometric measurement devices are expected to evolve over time, which may also have an impact on the measured series, especially measured precipitation extremes. For instance, saturation of the pluviograph shell-hole frequently occurred in the past sets an upper limit to the measure intensities over several minutes. In future studies, more studies should be conducted to improve the observation capabilities and bias correction methods for short-duration precipitation.
2. Reliable projections of future short-duration extreme precipitation are crucial for either developing climate-based IDF curves or analysis of future changes of short-duration precipitation. However, almost all the existing climate models do not consider the changes in urban underlying surface. For relatively large scale, changes of short-duration may be mainly dominated by climate change, while for urban areas the impacts of underlying surface changes cannot be neglected. To adequately characterize the urban environment in climate models, some researchers proposed introducing a parameterization scheme of urban canopy into climate models, and describing the links between the urban system and aerosols in climate models, and so on (Garuma, 2017; Jin & Shepherd, 2005; Pitman, Arneth, & Ganzeveld, 2012; Wang, Feng, Yan, Hu, & Jia, 2012). However, the influence of land cover has not been clearly demonstrated until now. Besides, to narrow the gap between local scale and the relative larger scale of climate models, bias correction of climate and meteorological models, including statistical and dynamic downscaling, is also a major issue and limiting factor. Thus, more research efforts would help to improve the capabilities of climate models in modeling the interaction between urban underlying and local atmosphere, and to improve the downscaling techniques.
3. Precipitation extremes are typically described by multi-attribute properties, such as intensity, duration, and volume. Hence, a univariate frequency analysis is inadequate to fully describe the dependence structure among different attributes (Jiang et al., 2019). Several studies have attempted to develop copula-based IDF curves using multivariate statistical approaches under stationary conditions (Ariff, Jemain, Ibrahim, & Zin, 2012; Bezak, Sraj, & Mikos, 2016; Singh & Zhang, 2007). Under nonstationary conditions, Vinnarasi and Dhanya (2019) derived the time-varying intensity-duration relationship to investigate the joint statistical properties of intensity and duration using dynamic Bayesian copula function. In future studies, additional studies would be needed to improve the understanding of relationship between intensity and duration of short-duration precipitation extremes using multivariate statistical approaches.
4. In the context of changing environment, urban infrastructures are expected to suffer different risk of failure during the service period or design life period due to the changing properties of short-duration extreme precipitation. Therefore, for both covariate-based nonstationary IDF curves and climate-model-based IDF curves, the updated IDF

curves should be linked with the design life of urban infrastructures to communicate risk under future climate. In hydrology community, several well-designed nonstationary design approaches have been proposed considering design lifespan of infrastructures, such as the DLL, ER, and ADLL methods, primarily for nonstationary flood design. However, the implementation of nonstationary models might introduce larger uncertainties. Thus, the trade-off between uncertainties and model complexity should be considered in the process of updating IDF curves (Koutsoyiannis & Montanari, 2014; Serinaldi & Kilsby, 2015). An alternative approach is to estimate the design values using stationary models and account for nonstationarity through a safety or correction factor (Vogel et al., 2011). In future studies, more efforts would be needed to test the existing methods worldwide and develop more rational design strategies for updating IDF curves.

ACKNOWLEDGMENTS

Great thanks are due to the editor and reviewers for their professional and constructive comments and revision suggestions, which are greatly helpful for the improvement of our manuscript.

CONFLICT OF INTEREST

The authors have declared no conflicts of interest for this article.

AUTHOR CONTRIBUTIONS

Lei Yan: Conceptualization; funding acquisition; writing-original draft. **Lihua Xiong:** Funding acquisition; investigation; writing-review and editing. **Cong Jiang:** Data curation; funding acquisition; methodology. **Mengjie Zhang:** Formal analysis; resources; validation. **Dong Wang:** Data curation. **Chong-Yu Xu:** Funding acquisition; validation; writing-review and editing.

DATA AVAILABILITY STATEMENT

The data that support the findings of this study are available from the corresponding author upon reasonable request.

ORCID

Lei Yan  <https://orcid.org/0000-0002-9859-1915>

RELATED WIREs ARTICLES

[Flood frequency analysis: the Bayesian choice](#)

[On return period and probability of failure in hydrology](#)

[Global atmospheric moisture transport associated with precipitation extremes: Mechanisms and climate change impacts](#)

REFERENCES

- Acero, F. J., Parey, S., García, J. A., & Dacunha-Castelle, D. (2018). Return level estimation of extreme rainfall over the Iberian Peninsula: Comparison of methods. *Water*, 10(2), 179. <https://doi.org/10.3390/w10020179>
- Acero, F. J., Parey, S., Hoang, T. T. H., Dacunha-Castelle, D., García, J. A., & Gallego, M. C. (2017). Non-stationary future return levels for extreme rainfall over Extremadura (southwestern Iberian Peninsula). *Hydrological Sciences Journal-Journal des Sciences Hydrologiques*, 62(9), 1394–1411. <https://doi.org/10.1080/02626667.2017.1328559>
- Agilan, V., & Umamahesh, N. V. (2015). Detection and attribution of non-stationarity in intensity and frequency of daily and 4-h extreme rainfall of Hyderabad, India. *Journal of Hydrology*, 530, 677–697. <https://doi.org/10.1016/j.jhydrol.2015.10.028>
- Agilan, V., & Umamahesh, N. V. (2016). Is the covariate based non-stationary rainfall IDF curve capable of encompassing future rainfall changes? *Journal of Hydrology*, 541, 1441–1455. <https://doi.org/10.1016/j.jhydrol.2016.08.052>
- Agilan, V., & Umamahesh, N. V. (2017). What are the best covariates for developing non-stationary rainfall intensity-duration-frequency relationship? *Advances in Water Resources*, 101, 11–22. <https://doi.org/10.1016/j.advwatres.2016.12.016>
- Anandhi, A., Frei, A., Pierson, D. C., Schneiderman, E. M., Zion, M. S., Lounsbury, D., & Matonse, A. H. (2011). Examination of change factor methodologies for climate change impact assessment. *Water Resources Research*, 47, W03501. <https://doi.org/10.1029/2010WR009104>
- Ariff, N. M., Jemain, A. A., Ibrahim, K., & Zin, W. Z. W. (2012). IDF relationships using bivariate copula for storm events in peninsular Malaysia. *Journal of Hydrology*, 470, 158–171. <https://doi.org/10.1016/j.jhydrol.2012.08.045>
- Ban, N., Schmidli, J., & Schär, C. (2015). Heavy precipitation in a changing climate: Does short-term summer precipitation increase faster? *Geophysical Research Letters*, 42(4), 1165–1172. <https://doi.org/10.1002/2014GL062588>
- Barbero, R., Fowler, H. J., Lentink, G., & Blenkinsop, S. (2017). Is the intensification of precipitation extremes with global warming better detected at hourly than daily resolutions? *Geophysical Research Letters*, 44(2), 974–983. <https://doi.org/10.1002/2016GL071917>

- Bayazit, M. (2015). Nonstationarity of hydrological records and recent trends in trend analysis: A state-of-the-art review. *Environmental Processes*, 2(3), 527–542. <https://doi.org/10.1007/s40710-015-0081-7>
- Ben Alaya, M. A., Zwiers, F. W., & Zhang, X. (2020). Probable maximum precipitation in a warming climate over North America in Can-RCM4 and CRCM5. *Climatic Change*, 158(3–4), 611–629. <https://doi.org/10.1007/s10584-019-02591-7>
- Berg, P., & Haerter, J. O. (2013). Unexpected increase in precipitation intensity with temperature—a result of mixing of precipitation types? *Atmospheric Research*, 119, 56–61. <https://doi.org/10.1016/j.atmosres.2011.05.012>
- Bertola, M., Viglione, A., & Blschl, G. (2019). Informed attribution of flood changes to decadal variation of atmospheric, catchment and river drivers in Upper Austria. *Journal of Hydrology*, 577, 123919. <https://doi.org/10.1016/j.jhydrol.2019.123919>
- Bezak, N., Sraj, M., & Mikos, M. (2016). Copula-based IDF curves and empirical rainfall thresholds for flash floods and rainfall-induced landslides. *Journal of Hydrology*, 541, 272–284. <https://doi.org/10.1016/j.jhydrol.2016.02.058>
- Blenkinsop, S., & Fowler, H. J. (2014) *An Hourly and Multi-hourly Extreme Precipitation Climatology for the UK and Long-term Changes in Extremes*. 2nd International Conference on Vulnerability and Risk Analysis and Management, and the 6th International Symposium on Uncertainty Modeling and Analysis (Liverpool, UK). doi: <https://doi.org/10.1061/9780784413609.139>.
- Boukhefifa, M., Meddi, M., & Gaume, E. (2018). Integrated Bayesian estimation of intensity-duration-frequency curves: Consolidation and extensive testing of a method. *Water Resources Research*, 54(10), 7459–7477. <https://doi.org/10.1029/2018WR023366>
- Chen, S., Xiong, L., Ma, Q., Kim, J. S., Chen, J., & Xu, C.-Y. (2020). Improving daily spatial precipitation estimates by merging gauge observation with multiple satellite-based precipitation products based on the geographically weighted ridge regression method. *Journal of Hydrology*, 589, 125156. <https://doi.org/10.1016/j.jhydrol.2020.125156>
- Chen, X., Hossain, F., & Leung, L. R. (2017). Probable maximum precipitation in the U.S. Pacific northwest in a changing climate. *Water Resources Research*, 53(11), 9600–9622. <https://doi.org/10.1002/2017WR021094>
- Cheng, L., & Aghakouchak, A. (2014). Nonstationary precipitation intensity-duration-frequency curves for infrastructure design in a changing climate. *Scientific Reports*, 4(1), 378–381. <https://doi.org/10.1038/srep07093>
- Clark, P., Roberts, N., Lean, H. W., Ballard, S. P., & Charlton-Perez, C. (2016). Convection-permitting models: A step-change in rainfall forecasting. *Meteorological Applications*, 23(2), 165–181. <https://doi.org/10.1002/met.1538>
- Colmet-Daage, A., Sanchez-Gomez, E., Ricci, S., Llovel, C., Borrell Estupina, V., Quintana-Seguí, P., ... Servat, E. (2018). Evaluation of uncertainties in mean and extreme precipitation under climate change for northwestern Mediterranean watersheds from high-resolution med and Euro-CORDEX ensembles. *Hydrology and Earth System Sciences*, 22, 673–687. <https://doi.org/10.5194/hess-22-673-2018>
- Cooley, D. (2013). Return periods and return levels under climate change. In A. Aghakouchak, D. Easterling, K. Hsu, S. Schubert, & S. Sorooshian (Eds.), *Extremes in a changing climate* (pp. 97–114). Dordrecht, Netherlands: Springer. https://doi.org/10.1007/978-94-007-4479-0_4
- Couto, F. T., Ducrocq, V., Salgado, R., & Costa, M. J. (2016). Numerical simulations of significant orographic precipitation in Madeira Island. *Atmospheric Research*, 169, Part A, 102–112. <https://doi.org/10.1016/j.atmosres.2015.10.002>
- CSA (Canadian Standards Association). (2010). *Technical guide - development, interpretation and use of rainfall intensity-duration-frequency (IDF) information: Guideline for Canadian water resources practitioners*. Ottawa: CSA Group.
- Du, T., Xiong, L., Xu, C.-Y., Gippel, C. J., Guo, S., & Liu, P. (2015). Return period and risk analysis of nonstationary low-flow series under climate change. *Journal of Hydrology*, 527, 234–250. <https://doi.org/10.1016/j.jhydrol.2015.04.041>
- Ducrocq, V., Davolio, S., Ferretti, R., Flamant, C., Santaner, V. H., Kalthoff, N., ... Wernli, H. (2016). Introduction to the HyMeX special issue on “advances in understanding and forecasting of heavy precipitation in the Mediterranean through the HyMeX SOP1 field campaign”. *Quarterly Journal of the Royal Meteorological Society*, 142(S1), 1–6. <https://doi.org/10.1002/qj.2856>
- Evans, J. P., & Westra, S. (2012). Investigating the mechanisms of diurnal rainfall variability using a regional climate model. *Journal of Climate*, 25(20), 7232–7247. <https://doi.org/10.1175/JCLI-D-11-00616.1>
- Feng, Z., Leung, L. R., Hagos, S., Houze, R. A., Burleyson, C. D., & Balaguru, K. (2016). More frequent intense and long-lived storms dominate the springtime trend in central US rainfall. *Nature Communications*, 7, 13429. <https://doi.org/10.1038/ncomms13429>
- Fischer, E. M., & Knutti, R. (2015). Anthropogenic contribution to global occurrence of heavy-precipitation and high-temperature extremes. *Nature Climate Change*, 5(6), 560–564. <https://doi.org/10.1038/s41467-018-06765-2>
- Fosser, G., Kendon, E. J., Stephenson, D., & Tucker, S. (2020). Convection-permitting models offer promise of more certain extreme rainfall projections. *Geophysical Research Letters*, 47, e2020GL088151. <https://doi.org/10.1029/2020GL088151>
- Fu, S., Li, D., Sun, J., Si, D., Ling, J., & Tian, F. (2016). A 31-year trend of the hourly precipitation over South China and the underlying mechanisms. *Atmospheric Science Letters*, 17(3), 216–222. <https://doi.org/10.1002/asl.645>
- Fujibe, F. (2013). Clausius-Clapeyron-like relationship in multidecadal changes of extreme short-term precipitation and temperature in Japan. *Atmospheric Science Letters*, 14(3), 127–132. <https://doi.org/10.1002/asl2.428>
- Ganguli, P., & Coulibaly, P. (2017). Does nonstationarity in rainfall require nonstationary intensity-duration-frequency curves? *Hydrology and Earth System Sciences*, 21(12), 6461–6483. <https://doi.org/10.5194/hess-21-6461-2017>
- Garuma, G. F. (2017). Review of urban surface parameterizations for numerical climate models. *Urban Climate*, 24, 830–851. <https://doi.org/10.1016/j.uclim.2017.10.006>
- Gaume, E. (2018). Flood frequency analysis: The Bayesian choice. *Wiley Interdisciplinary Reviews: Water*, 5, e1290. <https://doi.org/10.1002/wat2.1290>
- Golroudbary, V. R., Zeng, Y., Mannaerts, C. M., & Su, Z. (2019). Response of extreme precipitation to urbanization over The Netherlands. *Journal of Applied Meteorology and Climatology*, 58(4), 645–661. <https://doi.org/10.1175/JAMC-D-18-0180.1>

- Gu, X., Zhang, Q., Li, J., Singh, V. P., & Sun, P. (2019). Impact of urbanization on nonstationarity of annual and seasonal precipitation extremes in China. *Journal of Hydrology*, 575, 638–655. <https://doi.org/10.1016/j.jhydrol.2019.05.070>
- Guerreiro, S. B., Fowler, H. J., Barbero, R., Westra, S., Lenderink, G., Blenkinsop, S., ... Li, X. (2018). Detection of continental-scale intensification of hourly rainfall extremes. *Nature Climate Change*, 8(9), 803–807. <https://doi.org/10.1038/s41558-018-0245-3>
- Hanel, M., Pavlaskova, A., & Kysely, J. (2016). Trends in characteristics of sub-daily heavy precipitation and rainfall erosivity in The Czech Republic. *International Journal of Climatology*, 36(4), 1833–1845. <https://doi.org/10.1002/joc.4463>
- Hansen, J., Ruedy, R., Sato, M., & Lo, K. (2010). Global surface temperature change. *Reviews of Geophysics*, 48(4), RG4004. <https://doi.org/10.1029/2010RG000345>
- Hao, Z., & Singh, V. P. (2016). Review of dependence modeling in hydrology and water resources. *Progress in Physical Geography-Earth and Environment*, 40(4), 549–578. <https://doi.org/10.1177/030913316632460>
- Hassanzadeh, E., Nazemi, A., Adamowski, J., Nguyen, T., & Van-Nguyen, V. (2019). Quantile-based downscaling of rainfall extremes: Notes on methodological functionality, associated uncertainty and application in practice. *Advances in Water Resources*, 131, 103371. <https://doi.org/10.1016/j.advwatres.2019.07.001>
- Hassanzadeh, E., Nazemi, A., & Elshorbagy, A. (2014). Quantile-based downscaling of precipitation using genetic programming: Application to IDF curves in Saskatoon. *Journal of Hydrologic Engineering*, 19(5), 943–955. [https://doi.org/10.1061/\(ASCE\)HE.1943-5584.0000854](https://doi.org/10.1061/(ASCE)HE.1943-5584.0000854)
- Herath, S. M., Sarukkalige, R., & Nguyen, V. T. V. (2018). Evaluation of empirical relationships between extreme rainfall and daily maximum temperature in Australia. *Journal of Hydrology*, 556, 1171–1181. <https://doi.org/10.1016/j.jhydrol.2017.01.060>
- Hosseiniزاده‌تالائی, P., Tabari, H., & Willems, P. (2018). Precipitation intensity-duration-frequency curves for Central Belgium with an ensemble of EURO-CORDEX simulations, and associated uncertainties. *Atmospheric Research*, 200, 1–12. <https://doi.org/10.1016/j.atmosres.2017.09.015>
- Hu, Y., Liang, Z., Chen, X., Liu, Y., Wang, H., Yang, J., & Li, B. (2017). Estimation of design flood using EWT and ENE metrics and uncertainty analysis under non-stationary conditions. *Stochastic Environmental Research and Risk Assessment*, 31(10), 2617–2626. <https://doi.org/10.1007/s00477-017-1404-1>
- Hu, Y., Liang, Z., Singh, V. P., Zhang, X., Wang, J., Li, B., & Wang, H. (2018). Concept of equivalent reliability for estimating the design flood under non-stationary conditions. *Water Resources Management*, 32(3), 997–1011. <https://doi.org/10.1007/s11269-017-1851-y>
- IPCC. (2013). *Climate change 2013: The physical science basis, contribution of working group I to the fifth assessment report of the intergovernmental panel on climate change*. United Kingdom and New York: Cambridge University Press.
- Jakob, D., Karoly, D. J., & Seed, A. (2011). Non-stationarity in daily and sub-daily intense rainfall-part 1: Sydney, Australia. *Natural Hazards and Earth System Sciences*, 11(8), 2263–2271. <https://doi.org/10.5194/nhess-11-2263-2011>
- Jiang, C., Xiong, L., Yan, L., Dong, J., & Xu, C.-Y. (2019). Multivariate hydrologic design methods under nonstationary conditions and application to engineering practice. *Hydrology and Earth System Sciences*, 23(3), 1683–1704. <https://doi.org/10.5194/hess-23-1683-2019>
- Jiang, P., Gautam, M. R., Zhu, J., & Yu, Z. (2013). How well do the GCMs/RCMs capture the multi-scale temporal variability of precipitation in the southwestern United States? *Journal of Hydrology*, 479, 75–85. <https://doi.org/10.1016/j.jhydrol.2012.11.041>
- Jin, M., & Shepherd, J. M. (2005). Inclusion of urban landscape in a climate model-how can satellite data help. *Bulletin of the American Meteorological Society*, 86(5), 681–689. <https://doi.org/10.1175/BAMS-86-5-681>
- Kan, G., Zhang, M., Liang, K., Wang, H., Jiang, Y., Li, J., ... Li, C. (2016). Improving water quantity simulation & forecasting to solve the energy-water-food nexus issue by using heterogeneous computing accelerated global optimization method. *Applied Energy*, 210, 420–433. <https://doi.org/10.1016/j.apenergy.2016.08.017>
- Koutsoyiannis, D., & Montanari, A. (2014). Negligent killing of scientific concepts: The stationarity case. *Hydrological Science Journal*, 60 (7–8), 1174–1183. <https://doi.org/10.1080/02626667.2014.959959>
- Kuang, Y., Xiong, L., Yu, K., Liu, P., Xu, C.-Y., & Yan, L. (2018). Comparison of first-order and second-order derived moment approaches in estimating annual runoff distribution. *Journal of Hydrologic Engineering*, 23(8), 04018034. [https://doi.org/10.1061/\(ASCE\)HE.1943-5584.0001683](https://doi.org/10.1061/(ASCE)HE.1943-5584.0001683)
- Kunkel, K. E., Karl, T. R., Easterling, D. R., Redmond, K., Young, J., Yin, X., & Hennon, P. (2013). Probable maximum precipitation and climate change. *Geophysical Research Letters*, 40(7), 1402–1408. <https://doi.org/10.1002/grl.50334>
- Langhans, W., Schmidli, J., Fuhrer, O., Bieri, S., & Schar, C. (2013). Long-term simulations of thermally driven flows and orographic convection at convection-parameterizing and cloud-resolving resolutions. *Journal of Applied Meteorology and Climatology*, 52(6), 1490–1510. <https://doi.org/10.1175/JAMC-D-12-0167.1>
- Lehmann, E. A., Phatak, A., Stephenson, A., & Lau, R. (2016). Spatial modelling framework for the characterisation of rainfall extremes at different durations and under climate change. *Environmetrics*, 27(4), 239–251. <https://doi.org/10.1002/env.2389>
- Lenderink, G., & Fowler, H. J. (2017). Hydroclimate: Understanding rainfall extremes. *Nature Climate Change*, 7(6), 391–393. <https://doi.org/10.1038/nclimate3305>
- Lenderink, G., Mok, H. Y., Lee, T., & Van Oldenborgh, G. J. (2011). Scaling and trends of hourly precipitation extremes in two different climate zones-Hong Kong and The Netherlands. *Hydrology and Earth System Sciences*, 15(9), 3033–3041. <https://doi.org/10.5194/hess-15-3033-2011>
- Lenderink, G., & Van Meijgaard, E. (2008). Increase in hourly precipitation extremes beyond expectations from temperature changes. *Nature Geoscience*, 1(8), 511–514. <https://doi.org/10.1038/ngeo262>
- Li, J., Johnson, F., Evans, J., & Sharma, A. (2017). A comparison of methods to estimate future sub-daily design rainfall. *Advances in Water Resources*, 110, 215–227. <https://doi.org/10.1016/j.advwatres.2017.10.020>

- Liang, P., & Ding, Y. (2017). The long-term variation of extreme heavy precipitation and its link to urbanization effects in Shanghai during 1916–2014. *Advances in Atmospheric Sciences*, 34(3), 321–334. <https://doi.org/10.1007/s00376-016-6120-0>
- Lima, C. H. R., Kwon, H., & Kim, J. (2016). A Bayesian beta distribution model for estimating rainfall IDF curves in a changing climate. *Journal of Hydrology*, 540, 744–756. <https://doi.org/10.1016/j.jhydrol.2016.06.062>
- Lind, P., Belusic, D., Christensen, O. B., Dobler, A., Kjellstrom, E., Landgren, O., ... Wang, F. (2020). Benefits and added value of convection-permitting climate modeling over Fennoscandinavia. *Climate Dynamics*, 55, 1893–1912. <https://doi.org/10.1007/s00382-020-05359-3>
- Liu, B., Tan, X., Gan, T. Y., Chen, X., Lin, K., Lu, M., & Liu, Z. (2020). Global atmospheric moisture transport associated with precipitation extremes: Mechanisms and climate change impacts. *Wiley Interdisciplinary Reviews-Water*, 7(2), e1412. <https://doi.org/10.1002/wat2.1412>
- Liu, C., Ikeda, K., Rasmussen, R., Barlage, M., Newman, A. J., Prein, A. F., ... David, Y. (2017). Continental-scale convection-permitting modeling of the current and future climate of North America. *Climate Dynamics*, 49(1–2), 71–95. <https://doi.org/10.1007/s00382-016-3327-9>
- Lu, M., Xu, Y., Shan, N., Wang, Q., Yuan, J., & Wang, J. (2019). Effect of urbanisation on extreme precipitation based on nonstationary models in the Yangtze River Delta metropolitan region. *Science of the Total Environment*, 673, 64–73. <https://doi.org/10.1016/j.scitotenv.2019.03.413>
- Luke, A., Vrugt, J. A., AghaKouchak, A., Matthew, R., & Sanders, B. F. (2017). Predicting nonstationary flood frequencies: Evidence supports an updated stationarity thesis in the United States. *Water Resources Research*, 53(7), 5469–5494. <https://doi.org/10.1002/2016WR019676>
- Madsen, H., Arnbjerg-Nielsen, K., & Mikkelsen, P. S. (2009). Update of regional intensity-duration-frequency curves in Denmark: Tendency towards increased storm intensities. *Atmospheric Research*, 92(3), 343–349. <https://doi.org/10.1016/j.atmosres.2009.01.013>
- Mailhot, A., Duchesne, S., Caya, D., & Talbot, G. (2007). Assessment of future change in intensity-duration-frequency (IDF) curves for southern Quebec using the Canadian regional climate model (CRCM). *Journal of Hydrology*, 347(1), 197–210. <https://doi.org/10.1016/j.jhydrol.2007.09.019>
- Manola, I., van den Hurk, B., De Moel, H., & Aerts, J. C. J. H. (2018). Future extreme precipitation intensities based on a historic event. *Hydrology and Earth System Sciences*, 22, 3777–3788. <https://doi.org/10.5194/hess-22-3777-2018>
- Meinshausen, M., Meinshausen, N., Hare, W., Raper, S. C. B., Frieler, K., Knutti, R., ... Allen, M. R. (2009). Greenhouse-gas emission targets for limiting global warming to 2 °C. *Nature*, 458, 1158–1162. <https://doi.org/10.1038/nature08017>
- Miao, C., Sun, Q., Borthwick, A. G. L., & Duan, Q. (2016). Linkage between hourly precipitation events and atmospheric temperature changes over China during the warm season. *Scientific Reports*, 6, 22543. <https://doi.org/10.1038/srep22543>
- Mirhosseini, G., Srivastava, P., & Stefanova, L. (2013). The impact of climate change on rainfall intensity-duration-frequency (IDF) curves in Alabama. *Regional Environmental Change*, 13(1 Supplement), 25–33. <https://doi.org/10.1007/s10113-012-0375-5>
- Mishra, V., Ganguly, A. R., Nijssen, B., & Lettenmaier, D. P. (2015). Changes in observed climate extremes in global urban areas. *Environmental Research Letters*, 10(2), 024005. <https://doi.org/10.1088/1748-9326/10/2/024005>
- Montanari, A., & Koutsoyiannis, D. (2014). Modeling and mitigating natural hazards: Stationarity is immortal! *Water Resources Research*, 50(12), 9748–9756. <https://doi.org/10.1002/2014WR016092>
- Mure-Ravaud, M., Ishida, K., Kavvas, M. L., Yegorova, E., & Kanney, J. (2019). Numerical reconstruction of the intense precipitation and moisture transport fields for six tropical cyclones affecting the eastern United States. *Science of the Total Environment*, 665, 1111–1124. <https://doi.org/10.1016/j.scitotenv.2019.02.185>
- Mure-Ravaud, M., Kavvas, M. L., & Dib, A. (2019). Impact of increased atmospheric moisture on the precipitation depth caused by hurricane Ivan (2004) over a target area. *Science of the Total Environment*, 672, 916–926. <https://doi.org/10.1016/j.scitotenv.2019.03.471>
- Ngai, S. T., Tangang, F., & Juneng, L. (2017). Bias correction of global and regional simulated daily precipitation and surface mean temperature over Southeast Asia using quantile mapping method. *Global and Planetary Change*, 149, 79–90. <https://doi.org/10.1016/j.gloplacha.2016.12.009>
- Nguyen, V. T. V., Nguyen, T. D., & Cung, A. (2007). A statistical approach to downscaling of sub-daily extreme rainfall processes for climate-related impact studies in urban areas. *Water Science & Technology: Water Supply*, 7(2), 183–192. <https://doi.org/10.2166/ws.2007.053>
- Ntegeka, V., & Willems, P. (2008). Trends and multidecadal oscillations in rainfall extremes, based on a more than 100-year time series of 10 min rainfall intensities at Uccle, Belgium. *Water Resources Research*, 44(7), W07402. <https://doi.org/10.1029/2007WR006471>
- O'Gorman, P. A. (2015). Precipitation extremes under climate change. *Current Climate Change Reports*, 1(2), 49–59. <https://doi.org/10.1007/s40641-015-0009-3>
- Olsen, J. R., Lambert, J. H., & Haimes, Y. Y. (1998). Risk of extreme events under nonstationary conditions. *Risk Analysis*, 18(4), 497–510. <https://doi.org/10.1111/j.1539-6924.1998.tb00364.x>
- Ouarda, T. B. M. J., Yousef, L. A., & Charron, C. (2019). Non-stationary intensity-duration-frequency curves integrating information concerning teleconnections and climate change. *International Journal of Climatology*, 39(4), 2306–2323. <https://doi.org/10.1002/joc.5953>
- Parey, S., Hoang, T. T. H., & Dacunha-Castelle, D. (2010). Different ways to compute temperature return levels in the climate change context. *Environmetrics*, 21(7–8), 698–718. <https://doi.org/10.1002/env.1060>
- Parey, S., Malek, F., Laurent, C., & Dacunha-Castelle, D. (2007). Trends and climate evolution: Statistical approach for very high temperatures in France. *Climatic Change*, 81(3–4), 331–352. <https://doi.org/10.1007/s10584-006-9116-4>
- Pastén-Zapata, E., Jones, J. M., Moggridge, H., & Widmann, M. (2020). Evaluation of the performance of Euro-CORDEX regional climate models for assessing hydrological climate change impacts in Great Britain: A comparison of different spatial resolutions and quantile mapping bias correction methods. *Journal of Hydrology*, 584, 124653. <https://doi.org/10.1016/j.jhydrol.2020.124653>

- Pfahl, S., O'Gorman, P. A., & Fischer, E. M. (2017). Understanding the regional pattern of projected future changes in extreme precipitation. *Nature Climate Change*, 7, 423–427. <https://doi.org/10.1038/nclimate3287>
- Pingale, S. M., Khare, D., Jat, M. K., & Adamowski, J. (2014). Spatial and temporal trends of mean and extreme rainfall and temperature for the 33 urban centers of the arid and semi-arid state of Rajasthan, India. *Atmospheric Research*, 138, 73–90. <https://doi.org/10.1016/j.atmosres.2013.10.024>
- Pitman, A. J., Arneth, A., & Ganzeveld, L. (2012). Regionalizing global climate models. *International Journal of Climatology*, 32(3), 321–337. <https://doi.org/10.1002/joc.2279>
- Prein, A. F., Langhans, W., Fosser, G., Ferrone, A., Ban, N., Goergen, K., ... Leung, R. (2015). A review on regional convection-permitting climate modeling: Demonstrations, prospects, and challenges. *Reviews of Geophysics*, 53(2), 323–361. <https://doi.org/10.1002/2014RG000475>
- Prein, A. F., Rasmussen, R. M., Ikeda, K., Liu, C., Clark, M. P., & Holland, G. J. (2017). The future intensification of hourly precipitation extremes. *Nature Climate Change*, 7(1), 48–52. <https://doi.org/10.1038/nclimate3168>
- Pui, A., Sharma, A., Mehrotra, R., Sivakumar, B., & Jeremiah, E. (2012). A comparison of alternatives for daily to sub-daily rainfall disaggregation. *Journal of Hydrology*, 470–471, 138–157. <https://doi.org/10.1016/j.jhydrol.2012.08.041>
- Qu, C., Li, J., Yan, L., Yan, P., & Lu, D. (2020). Non-stationary flood frequency analysis using cubic B-spline-based gammss model. *Water*, 12(7), 1867. <https://doi.org/10.3390/w12071867>
- Ragno, E., Aghakouchak, A., Love, C. A., Cheng, L., Vahedifard, F., & Lima, C. H. R. (2018). Quantifying changes in future intensity-duration-frequency curves using multimodel ensemble simulations. *Water Resources Research*, 54(3), 1751–1764. <https://doi.org/10.1002/2017WR021975>
- Rigby, R. A., & Stasinopoulos, D. (2005). Generalized additive models for location, scale and shape. *Journal of the Royal Statistical Society Series C-Applied Statistics*, 54(3), 507–554. <https://doi.org/10.1111/j.1467-9876.2005.00510.x>
- Rootzén, H., & Katz, R. W. (2013). Design life level: Quantifying risk in a changing climate. *Water Resources Research*, 49(9), 5964–5972. <https://doi.org/10.1002/wrcr.20425>
- Salas, J. D., & Obeysekera, J. (2014). Revisiting the concepts of return period and risk for nonstationary hydrologic extreme events. *Journal of Hydrologic Engineering*, 19(3), 554–568. [https://doi.org/10.1061/\(ASCE\)HE.1943-5584.0000820](https://doi.org/10.1061/(ASCE)HE.1943-5584.0000820)
- Salas, J. D., Obeysekera, J., & Vogel, R. M. (2018). Techniques for assessing water infrastructure for nonstationary extreme events: A review. *Hydrological Sciences Journal-Journal des Sciences Hydrologiques*, 63(3), 325–352. <https://doi.org/10.1080/02626667.2018.1426858>
- Sarhadi, A., & Soulis, E. D. (2017). Time-varying extreme rainfall intensity-duration-frequency curves in a changing climate. *Geophysical Research Letters*, 44(5), 2454–2463. <https://doi.org/10.1002/2016GL072201>
- Sauvage, C., Brossier, C. L., Bouin, M.-N., & Ducrocq, V. (2020). Characterization of the air-sea exchange mechanisms during a Mediterranean heavy precipitation event using realistic sea state modelling. *Atmospheric Chemistry and Physics*, 20(3), 1675–1699. <https://doi.org/10.5194/acp-20-1675-2020>
- Schiemann, R., Vidale, P. L., Shaffrey, L. C., Johnson, S. J., Roberts, M. J., Demory, M.-E., ... Strachan, J. (2018). Mean and extreme precipitation over European river basins better simulated in a 25 km AGCM. *Hydrology and Earth System Sciences*, 22, 3933–3950. <https://doi.org/10.5194/hess-22-3933-2018>
- Semadeni-Davies, A., Hernebring, C., Svensson, G., & Gustafsson, L. (2008). The impacts of climate change and urbanisation on drainage in Helsingborg, Sweden: Combined sewer system. *Journal of Hydrology*, 350(1–2), 100–113. <https://doi.org/10.1016/j.jhydrol.2007.05.028>
- Serinaldi, F., & Kilsby, C. G. (2015). Stationarity is undead: Uncertainty dominates the distribution of extremes. *Advances in Water Resources*, 77, 17–36. <https://doi.org/10.1016/j.advwatres.2014.12.013>
- Sharif, M., & Burn, D. H. (2007). Improved k-nearest neighbor weather generating model. *Journal of Hydrologic Engineering*, 12(1), 42–51. [https://doi.org/10.1061/\(ASCE\)1084-0699\(2007\)12:1\(42\)](https://doi.org/10.1061/(ASCE)1084-0699(2007)12:1(42))
- Singh, V. P., & Zhang, L. (2007). IDF curves using the frank Archimedean copula. *Journal of Hydrologic Engineering*, 12(6), 651–662. [https://doi.org/10.1061/\(ASCE\)1084-0699\(2007\)12:6\(651\)](https://doi.org/10.1061/(ASCE)1084-0699(2007)12:6(651))
- Siswanto, S., Van Oldenborgh, G. J., Der Schrier, G. V., Jilderda, R., & Van Den Hurk, B. (2016). Temperature, extreme precipitation, and diurnal rainfall changes in the urbanized Jakarta city during the past 130 years. *International Journal of Climatology*, 36(9), 3207–3225. <https://doi.org/10.1002/joc.4548>
- Srivastav, R. K., Schardong, A., & Simonovic, S. P. (2014). Equidistance quantile matching method for updating IDF curves under climate change. *Water Resources Management*, 28(9), 2539–2562. <https://doi.org/10.1007/s11269-014-0626-y>
- Syafrina, A. H., Zalina, M. D., & Juneng, L. (2015). Historical trend of hourly extreme rainfall in peninsular Malaysia. *Theoretical and Applied Climatology*, 120(1–2), 259–285. <https://doi.org/10.1007/s00704-014-1145-8>
- Trenberth, K. E. (1999). Conceptual framework for changes of extremes of the hydrological cycle with climate change. *Climatic Change*, 42(1), 327–339. <https://doi.org/10.1023/A:1005488920935>
- Tripathi, O. P., & Dominguez, F. (2013). Effects of spatial resolution in the simulation of daily and subdaily precipitation in the southwestern U.S. *Journal of Geophysical Research*, 118(14), 7591–7605. <https://doi.org/10.1002/jgrd.50590>
- Um, M., Kim, Y., Markus, M., & Wuebbles, D. J. (2017). Modeling nonstationary extreme value distributions with nonlinear functions: An application using multiple precipitation projections for U.S. cities. *Journal of Hydrology*, 552, 396–406. <https://doi.org/10.1016/j.jhydrol.2017.07.007>
- Viglione, A., Merz, R., Salinas, J. L., & Bloeschl, G. (2013). Flood frequency hydrology: 3. A Bayesian analysis. *Water Resources Research*, 49(2), 675–692. <https://doi.org/10.1029/2011WR010782>
- Villarini, G., Serinaldi, F., Smith, J. A., & Krajewski, W. F. (2009). On the stationarity of annual flood peaks in the continental United States during the 20th century. *Water Resources Research*, 45(8), W08417. <https://doi.org/10.1029/2008WR007645>

- Vinnarasi, R., & Dhanya, C. T. (2019). Bringing realism into a dynamic copula-based non-stationary intensity-duration model. *Advances in Water Resources*, 130, 325–338. <https://doi.org/10.1016/j.advwatres.2019.06.009>
- Vogel, R. M., Yaindl, C., & Walter, M. (2011). Nonstationarity: Flood magnification and recurrence reduction factors in the united States1. *Journal of the American Water Resources Association*, 47(3), 464–474. <https://doi.org/10.1111/j.1752-1688.2011.00541.x>
- Volpi, E. (2019). On return period and probability of failure in hydrology. *Wiley Interdisciplinary Reviews: Water*, 6(3), e1340. <https://doi.org/10.1002/wat2.1340>
- Wang, J., Feng, J., Yan, Z., Hu, Y., & Jia, G. (2012). Nested high-resolution modeling of the impact of urbanization on regional climate in three vast urban agglomerations in China. *Journal of Geophysical Research*, 117, D21103. <https://doi.org/10.1029/2012JD018226>
- Wasko, C., Sharma, A., & Johnson, F. (2015). Does storm duration modulate the extreme precipitation-temperature scaling relationship? *Geophysical Research Letters*, 42(20), 8783–8790. <https://doi.org/10.1002/2015GL066274>
- Westra, S., Alexander, L. V., & Zwiers, F. W. (2013). Global increasing trends in annual maximum daily precipitation. *Journal of Climate*, 26 (11), 3904–3918. <https://doi.org/10.1175/JCLI-D-12-00502.1>
- Westra, S., Fowler, H. J., Evans, J. P., Alexander, L. V., Berg, P., Johnson, F., ... Roberts, N. M. (2014). Future changes to the intensity and frequency of short-duration extreme rainfall. *Reviews of Geophysics*, 52(3), 522–555. <https://doi.org/10.1002/2014RG000464>
- Willems, P. (2013). Revision of urban drainage design rules after assessment of climate change impacts on precipitation extremes at Uccle, Belgium. *Journal of Hydrology*, 496, 166–177. <https://doi.org/10.1016/j.jhydrol.2013.05.037>
- Willems, P., ArnbjergNielsen, K., Olsson, J., & Nguyen, V. (2012). Climate change impact assessment on urban rainfall extremes and urban drainage: Methods and shortcomings. *Atmospheric Research*, 103, 106–118. <https://doi.org/10.1016/j.atmosres.2011.04.003>
- Xiong, B., Xiong, L., Guo, S., Xu, C.-Y., Xia, J., Zhong, Y., & Yang, H. (2020). Nonstationary frequency analysis of censored data: A case study of the floods in the Yangtze River from 1470 to 2017. *Water Resources Research*, 56, e2020WR027112. <https://doi.org/10.1029/2020WR027112>
- Xiong, L., Yan, L., Du, T., Yan, P., Li, L., & Xu, W. (2019). Impacts of climate change on urban extreme rainfall and drainage infrastructure performance: A case study in Wuhan City, China. *Irrigation and Drainage*, 68(2), 152–164. <https://doi.org/10.1002/ird.2316>
- Xu, W., Jiang, C., Yan, L., Li, L., & Liu, S. (2018). An adaptive metropolis-Hastings optimization algorithm of Bayesian estimation in non-stationary flood frequency analysis. *Water Resources Management*, 32(4), 1343–1366. <https://doi.org/10.1007/s11269-017-1873-5>
- Yan, L., Li, L., Yan, P., He, H., Li, J., & Lu, D. (2019). Nonstationary flood hazard analysis in response to climate change and population growth. *Water*, 11(9), 1811. <https://doi.org/10.3390/w11091811>
- Yan, L., Xiong, L., Guo, S., Xu, C.-Y., Xia, J., & Du, T. (2017). Comparison of four nonstationary hydrologic design methods for changing environment. *Journal of Hydrology*, 551, 132–150. <https://doi.org/10.1016/j.jhydrol.2017.06.001>
- Yan, L., Xiong, L., Liu, D., Hu, T., & Xu, C.-Y. (2017). Frequency analysis of nonstationary annual maximum flood series using the time-varying two-component mixture distributions. *Hydrological Processes*, 31(1), 69–89. <https://doi.org/10.1002/hyp.10965>
- Yan, L., Xiong, L., Luan, Q., Jiang, C., Yu, K., & Xu, C.-Y. (2020). On the applicability of the expected waiting time method in nonstationary flood design. *Water Resources Management*, 34(8), 2585–2601. <https://doi.org/10.1007/s11269-020-02581-w>
- Yan, L., Xiong, L., Ruan, G., Xu, C.-Y., Yan, P., & Liu, P. (2019). Reducing uncertainty of design floods of two-component mixture distributions by utilizing flood timescale to classify flood types in seasonally snow covered region. *Journal of Hydrology*, 574, 588–608. <https://doi.org/10.1016/j.jhydrol.2019.04.056>
- Yang, H., Xiong, L., Xiong, B., Zhang, Q., & Xu, C.-Y. (2020). Separating runoff change by the improved budyko complementary relationship considering effects of both climate change and human activities on basin characteristics. *Journal of Hydrology*, 591, 125330. <https://doi.org/10.1016/j.jhydrol.2020.125330>
- Yang, Y., Smith, J. A., Yang, L., Baeck, M. L., & Ni, G. (2019). Regional impacts of urban irrigation on surface heat fluxes and rainfall in Central Arizona. *Journal of Geophysical Research Atmospheres*, 124(12), 6393–6410. <https://doi.org/10.1029/2018JD030213>
- Zahmatkesh, Z., Karamouz, M., Goharian, E., & Burian, S. J. (2015). Analysis of the effects of climate change on urban storm water runoff using statistically downscaled precipitation data and a change factor approach. *Journal of Hydrologic Engineering*, 20(7), 5014022. [https://doi.org/10.1061/\(ASCE\)HE.1943-5584.0001064](https://doi.org/10.1061/(ASCE)HE.1943-5584.0001064)
- Zhang, W., Villarini, G., Vecchi, G. A., & Smith, J. A. (2018). Urbanization exacerbated the rainfall and flooding caused by hurricane Harvey in Houston. *Nature*, 563(7731), 384–388. <https://doi.org/10.1038/s41586-018-0676-z>
- Zhang, X., Zwiers, F. W., Li, G., Wan, H., & Cannon, A. J. (2017). Complexity in estimating past and future extreme short-duration rainfall. *Nature Geoscience*, 10(4), 255–259. <https://doi.org/10.1038/ngeo2911>
- Zhou, X., Bai, Z., & Yang, Y. (2017). Linking trends in urban extreme rainfall to urban flooding in China. *International Journal of Climatology*, 37(13), 4586–4593. <https://doi.org/10.1002/joc.5107>
- Zittis, G., Bruggeman, A., Camera, C., Hadjinicolaou, P., & Lelieveld, J. (2017). The added value of convection permitting simulations of extreme precipitation events over the eastern Mediterranean. *Atmospheric Research*, 191, 20–33. <https://doi.org/10.1016/j.atmosres.2017.03.002>

How to cite this article: Yan L, Xiong L, Jiang C, Zhang M, Wang D, Xu C-Y. Updating intensity-duration-frequency curves for urban infrastructure design under a changing environment. *WIREs Water*. 2021;8:e1519. <https://doi.org/10.1002/wat2.1519>